On the long time behaviour of single stochastic Hodgkin-Huxley neurons with constant signal, and a construction of circuits of interacting neurons showing self-organized rhythmic oscillations

Reinhard Höpfner*

Abstract

The stochastic Hodgkin-Huxley neurons considered in this paper replace time-constant deterministic input adt of the classical deterministic model by increments $\vartheta dt + dX_t$ of a stochastic process: X is Ornstein-Uhlenbeck with volatility $\sigma > 0$ and back-driving force $\tau > 0$, and we call $\vartheta > 0$ the signal. We have ergodicity and strong laws of large numbers for various functionals of the process, and characterize 'quiet behaviour' and 'regular spiking' as events whose probability depends on the parameters (τ, σ) and on the signal ϑ. The notions of quiet behaviour and regular spiking allow for a construction of circuits of interacting stochastic Hodgkin-Huxley neurons, combining excitation with inhibition according to a block structure along the circuit, on which self-organized rhythmic oscillations can be observed. .

1 Introduction

Self-organized rhythmic oscillation in stochastic systems has been studied in different contexts in biology and physics. Cerf, Dai Pra, Formentin and Tovazzi [3] study spin systems with nearest neighbour interaction along a circuit which show the following behaviour. Starting from magnetisation (all spins equal to 1, say) a rather long waiting time is needed to observe flipping of a first spin, rapidly followed –in virtue of the structure of the interaction– by spins flipping at successive neighbouring sites along the circuit which leads to magnetisation of opposite sign (all spins equal to -1, say). Then again, with roles of signs interchanged, a rather long time is needed to observe a first spin flipping back, rapidly followed by successive neighbours, and the circuit returns to its initial state of magnetization. This creates a self-organized rhythmic oscillation in a Markovian system which is homogeneous in time. The authors can prove that this oscillation is persistent.

*Inst. für Mathematik, Johannes Gutenberg Univ. Mainz, E-mail: hoepfner@mathematik.uni-mainz.de

On the long time behaviour of stochastic Hodgkin-Huxley neurons

Ditlevsen and Löcherbach [4] study circuits of blocks of neurons –where interaction between successive blocks is of mean-field type– where neurons are modelled through Hawkes processes, i.e. Poissonian point processes where intensity is a function of past spiking activity in preceding blocks. Non-Markovian in general, specific memory kernels however allow an expansion of the structure into Markovian cascades, *i.e.* finite sequences of successive Markovian steps corresponding to every block. Now Markovian ergodicity tools are again at hand, together with mean field limits in large blocks. When inhibition and excitation is properly balanced, the authors prove that in the limit the circuit behaves as a deterministic system enjoying the following properties (Theorem 3 in Section 4 of [4]): i) exactly one equilibrium point exists for the system; ii) this equilibrium point is unstable, iii) there is a stable periodic orbit for the system; iv) other periodic orbits may exist, but at most in finite number.

The aim of the present paper is to show that similar patterns of self-organized rhythmic oscillation can be observed in the spike trains of certain circuits of interacting stochastic Hodgkin-Huxley neurons, under suitable balance of excitation and inhibition according to a block structure in the circuit, and under careful determination of suitable 'levels of noise'.

In this view, a first ingredient is to work out, for single stochastic Hodgkin-Huxley neurons receiving input $\vartheta dt + dX_t$ where X is an Ornstein-Uhlenbeck process with back-driving force $\tau > 0$ and volatility $\sigma > 0$, a notion of 'quiet behaviour' and a notion of 'regular spiking' such that, for suitable pairs (τ, σ) characterizing the level of 'noise' and with large probability, 'regular spiking' will be observed for suitably large values ϑ_2 of the signal, and 'quiet behaviour' for suitably small values ϑ_1. Quiet behaviour on a time interval of certain length will be defined through a comparison with Poisson processes of very low intensity, and regular spiking in terms of quantiles of interspike times clustering around their median. Simulations provide evidence that it is not sufficient to choose the signal alone strong enough (*e.g.*, such that trajectories of a deterministic Hodgkin-Huxley neuron with constant input would be attracted by a stable orbit, for almost all initial conditions, in presence of an unstable equilibrium point), or the signal alone weak enough (*e.g.*, such that trajectories of a deterministic Hodgkin-Huxley neuron with constant input would be attracted by a stable fixed point, for almost all initial conditions): the essential condition in stochastic neurons is an interplay, in dependence on suitable pairs of values $\vartheta_1 < \vartheta_2$ for the signal, between volatility (sufficiently small) and back-driving force (sufficiently strong).

The second ingredient is to associate to every neuron in the circuit an output process, solution to an Ornstein-Uhlenbeck type SDE driven by the point process of its spikes, with positive back-driving force. We have to transform this output into input for a successor neuron. In a circuit of $N = ML$ neurons, ordered in M blocks containing L neurons each, and where we count neurons modulo N around the circuit, the output of neuron $i-1$ transforms into input for neuron i in the following way: neurons which occupy first positions in their respective blocks receive bounded inhibitory input, neurons having their predecessor in the same block (*i.e.* all others) receive bounded excitatory input. With suitable choice of bounded monotone functions Φ_{inh} (decreasing) and Φ_{exc} (increasing), writing $U^{(j)}$ for the output produced by neuron j, the input which neuron i receives is thus

$$\Phi_{\text{inh}}(U^{(i-1)}) \quad \text{if } i = 1 \quad \text{modulo} \quad L, \quad \Phi_{\text{exc}}(U^{(i-1)}) \quad \text{else}$$

(in particular, neuron 1 receives input $\Phi_{\text{inh}}(U^{(N)})$, counting modulo N around the circuit). Suitably balanced and under the condition that the number M of blocks is odd, simulations make appear oscillating patterns of spiking activity around the circuit in the sense that blocks of neurons flip from regular spiking regime into quiet regime and

from quiet regime into regular spiking regime. This creates a slow rhythmic oscillation of activity patterns around the circuit which seems persistent. Simulation results as represented in Figures 7 and 8 illustrate this phenomenon, already for small values of L and M, and show that rhythmic oscillation establishes itself rather rapidly.

We have no proof that the observed slow rhythmic oscillation of spiking activity around the circuit is indeed persistent. A heuristic argument however might be as follows. Think of a deterministic system of dimension $N = LM$ where variables $t \to x_j(t)$ represent in some way a spiking activity of neuron j as a function of time, and where counting modulo N the interaction scheme is of type

$$\frac{dx_i}{dt}(t) = \begin{cases} -cx_i(t) - f(x_{i-1}(t)) & \text{if} \quad i = 1 \quad \text{modulo} \quad L \\ -cx_i(t) + f(x_{i-1}(t)) & \text{else} \end{cases}$$

with f some smooth function which is close to the truncation function $x \to (x \vee -1) \wedge 1$, and with $c > 0$ some constant. Under the condition that i) M is odd and ii) c is small enough, this system evolves on a finite number of periodic orbits, and at least one periodic orbit is stable. This is again Theorem 3 in section 4 of [4], the system $t \to (x_1(t), \ldots, x_N(t))$ being a simplified version of the deterministic limit system considered there. In simulations under random initial conditions, the slow rhythmic oscillation of activity patterns in the circuit of stochastic Hodgkin-Huxley neurons constructed above looks very much like those in the deterministic system $t \to (x_1(t), \ldots, x_N(t))$.

The main effort of the present paper is on modelization and balance, a key ingredient being a rigorous definition of notions such as quiet behaviour and regular spiking in stochastic Hodgkin-Huxley neurons with constant signal. Proofs that the oscillating behaviour observed in finite circuits of stochastic Hodgkin-Huxley neurons is indeed persistent (certainly perturbed by randomness from time to time but always re-establishing itself rather rapidly) remains an open and challenging problem.

The present paper is organized as follows. At the core of the paper, Section 6 is devoted to the construction of circuits which exhibit self-organized oscillation. This section does not contain proofs. As a preparation for Section 6, all other sections except the first one (which recalls some known facts for classical deterministic Hodgkin-Huxley neurons with constant input) focus on the single stochastic Hodgkin-Huxley neuron as a Harris recurrent strong Markov process.

In particular, Section 3 introduces the stochastic Hodgkin-Huxley neuron with constant signal, sketches its ergodicity properties and states some strong laws of large numbers, in particular for empirical distribution functions of spiking patterns. Proofs based on artificially defined life cycles through Nummelin splitting (methods as in Höpfner, Löcherbach and Thieullen [11, 12, 13]) are collected in an appendix Section 7. The process of 'output' of a stochastic neuron, key tool in view of modelization of interactions along circuits, is defined in Section 3.3. Quantifying a comparison with Poisson processes of very low intensity, Section 4 defines quiet behaviour of a single stochastic Hodgkin-Huxley neuron with constant signal as an event whose probability depends on the noise level and the value of the signal. Section 5 defines regular spiking in terms of quantiles of interspike times which cluster sufficiently close to their median. Consequences for the output process (based on two conjectures –which we believe realistic– on concentration properties of the limit of empirical distribution function for interspike times) are discussed in an appendix Section 8.

The limit theorems of Section 3 and the notions in Sections 4–5 form the basis for the construction of circuits of interacting stochastic Hodgkin-Huxley neurons in Section 6, whereas Appendices 7–8 may be left for further reading.

R code underlying our simulations in the present paper is provided under http://modeldb.yale.edu/267611.

2 Deterministic Hodgkin-Huxley model with constant rate of input

Hodgkin-Huxley models [6] play an important role in neuroscience and are considered as realistic models for the spiking behaviour of neurons. For an overview see Izhikevich [15] and Ermentrout and Terman [5]. The classical deterministic model with constant rate of input is a 4-dimensional dynamical system with variables (V, n, m, h)

$$\begin{cases} dV_t = a\,dt - F(V_t, n_t, m_t, h_t)dt \\ dn_t = [\alpha_n(V_t)(1 - n_t) - \beta_n(V_t)n_t]dt \\ dm_t = [\alpha_m(V_t)(1 - m_t) - \beta_m(V_t)m_t]dt \\ dh_t = [\alpha_h(V_t)(1 - h_t) - \beta_h(V_t)h_t]dt \end{cases} \tag{2.1}$$

where $a > 0$ is a constant. We define the functions F and α_j, β_j, $j \in \{n, m, h\}$, as in Izhikevich [15, pp. 37–38] (different choices for the constants exist in the literature):

$$F(v, n, m, h) := 36n^4(v + 12) + 120m^3h(v - 120) + 0.3(v - 10.6), \tag{2.2}$$

$$\alpha_n(v) = \frac{0.1 - 0.01v}{\exp(1 - 0.1v) - 1} \qquad \beta_n(v) = 0.125\exp(-v/80),$$

$$\alpha_m(v) = \frac{2.5 - 0.1v}{\exp(2.5 - 0.1v) - 1} \qquad \beta_m(v) = 4\exp(-v/18), \tag{2.3}$$

$$\alpha_h(v) = 0.07\exp(-v/20) \qquad \beta_h(v) = \frac{1}{\exp(3 - 0.1v) + 1}.$$

The variable V takes values in $\mathbb{R}$ and models the membrane potential in the single neuron. The variables n, m, h are termed gating variables (or internal variables) and take values in $[0, 1]$. The state space for this system is $E_4 := \mathbb{R} \times [0, 1]^3$. In the sequel, for reasons which will appear in Section 3, we shall speak of $a > 0$ in (2.1) as a 'signal' and try to avoid the term 'input rate' established in the literature on deterministic Hodgkin-Huxley models.

Depending on the value of the signal $a > 0$, the following behaviour of the deterministic dynamical system is known, see Ermentrout and Terman [5, pp. 63–66]. As there, see (2.4) and (2.5) below, (2.1) admits a unique equilibrium for every $a > 0$. On some interval $(0, a_1)$ this equilibrium point is stable. There is a bistability interval $\mathbb{I}_{bs} = (a_1, a_2)$ on which a stable orbit coexists with a stable equilibrium point, and an interval (a_2, a_3) on which the orbit is stable whereas the equilibrium point is unstable. As a approaches from below the right endpoint a_3 of the last interval, orbits are collapsing towards equilibrium; for $a > a_3$ the equilibrium point is again stable. Here $0 < a_1 < a_2 < a_3 < \infty$ are suitably determined endpoints for intervals. Equilibrium points and orbits depend on the value of a. For biologically relevant values of the signal, evolution of the system along an orbit represents a remarkably fast 'large excursion' of all variables of the system, in particular of the membrane potential V, and is called a spike. Throughout the paper, we exclude unrealistically large values of the signal.

In simulations –Euler schemes with time step 0.001 where the starting point is selected at random, according to the uniform law on $(-12, 120) \times (0, 1)^3$– the equilibrium point appears to be globally attractive on $(0, a_1)$. The orbit appears to be globally attractive on (a_2, a_3). On the bistability interval $\mathbb{I}_{bs} = (a_1, a_2)$, the behaviour of the system depends on the choice of the starting value: simulated trajectories either go to the equilibrium point, or are attracted by the orbit.[1]

---

[1]Rinzel and Miller [22] show that a branch of unstable periodic orbits exists on the bistability interval, bifurcating below $a_2 = \sup \mathbb{I}_{bs}$ and rejoining the stable orbits at $a_1 = \inf \mathbb{I}_{bs}$ (in the sense of decreasing values of a). However, such orbits will not be seen in simulations with randomly chosen starting point.

For our choice of the constants in equations (2.2)–(2.3) –those of Izhikevich [15], slightly different from both Ermentrout and Terman [5] and Rinzel and Miller [22]– simulations (here we refer to those[2] done by [14]) locate $\inf \mathbb{I}_{\mathrm{bs}} = a_1$ between 5.24 and 5.25, and $\sup \mathbb{I}_{\mathrm{bs}} = a_2$ close to 8.4 . The value of a_3 is close to 163.5 and thus (given the shape of orbits when a approaches a_3 from below) far beyond biological relevance. Already at $a = 5.5$, about 80% of all trajectories with randomly selected starting point are attracted to the orbit, this percentage being increasing in $a \in \mathbb{I}_{\mathrm{bs}}$.

Equilibria for the deterministic Hodgkin-Huxley system (2.1) can be determined as follows ([15, pp. 38–39], and [5]). For a fixed value v of the membrane potential, write

$$(n_\infty(v), m_\infty(v), h_\infty(v)) := \left(\frac{\alpha_n}{\alpha_n + \beta_n}(v), \frac{\alpha_m}{\alpha_m + \beta_m}(v), \frac{\alpha_h}{\alpha_h + \beta_h}(v) \right) \qquad (2.4)$$

and define $F_\infty : \mathbb{R} \to \mathbb{R}$ by

$$F_\infty(v) := F(v, n_\infty(v), m_\infty(v), h_\infty(v)). \qquad (2.5)$$

Numerical evidence (see also the remarks in [5, pp. 64–65]) shows that F_∞ is strictly increasing on compacts. Thus, for signal $a > 0$ in (2.1)–(2.3), solving

$$a \stackrel{!}{=} F_\infty(v^{\{a\}})$$

we determine $v^{\{a\}}$ and thus the equilibrium point

$$\left(v^{\{a\}}, n^{\{a\}}, m^{\{a\}}, h^{\{a\}} \right) := \left(v^{\{a\}}, n_\infty(v^{\{a\}}), m_\infty(v^{\{a\}}), h_\infty(v^{\{a\}}) \right) \qquad (2.6)$$

of the deterministic system (2.1) with signal $a > 0$.

3 Stochastic Hodgkin-Huxley with constant signal

Prepare an Ornstein-Uhlenbeck process with back-driving force $\tau > 0$ and volatility $\sigma > 0$

$$dX_t = -\tau X_t dt + \sigma dW_t. \qquad (3.1)$$

---

[2]In unpublished work [14], Hummel simulated 1000 trajectories with randomly selected starting point for each value of the signal a under consideration. Starting values were sampled independently from the uniform law on $(-12, 120) \times (0, 1)^3$. As a function of a (given in the first row of the tables below), the following relative number (given in the second row) of trajectories was found to converge to an orbit. First, for a in $[8.0, 9.0)$,

8.0	8.1	8.2	8.3	8.4	8.5	8.6	8.7	8.8	8.9
0.986	0.991	0.993	0.998	1.000	1.000	1.000	1.000	1.000	1.000

which determines an approximate location ≈ 8.4 of the right endpoint of $\mathbb{I}_{\mathrm{bs}}$. Then, considering values of a in $[5.0, 6.0)$

5.0	5.1	5.2	5.3	5.4	5.5	5.6	5.7	5.8	5.9
0.000	0.000	0.000	0.751	0.777	0.803	0.821	0.835	0.847	0.863

and looking in more detail into the interval $[5.2, 5.3)$

5.20	5.21	5.22	5.23	5.24	5.25	5.26	5.27	5.28	5.29
0.000	0.000	0.000	0.000	0.000	0.687	0.726	0.736	0.743	0.748

the left endpoint of $\mathbb{I}_{\mathrm{bs}}$ is found between 5.24 and 5.25; a closer look into $[5.24, 5.25)$

5.240	5.241	5.242	5.243	5.244	5.245	5.246	5.247	5.248	5.249
0.000	0.012	0.073	0.134	0.214	0.294	0.368	0.435	0.547	0.653

shows that $\inf \mathbb{I}_{\mathrm{bs}}$ is in fact very close to 5.24. All values above are quoted from [14], p. 10 there.
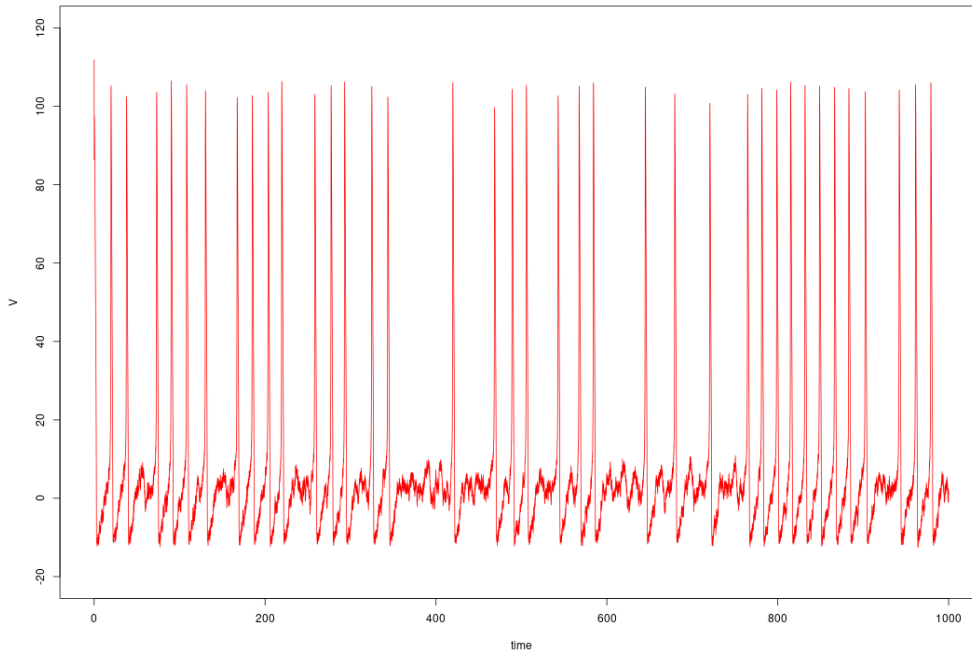
Figure 1: Membrane potential in a simulated stochastic Hodgkin-Huxley neuron $\mathbb{X}^{(\vartheta,\tau,\sigma)}$. The value of the signal is $\vartheta = 4$, and the parameters for the Ornstein Uhlenbeck process X are $\tau = 0.5$ and $\sigma = 2.5$. Initial conditions are selected at random, according to the stationary law of X and according to the uniform law on $(-12, 120) \times (0, 1)^3$ for (V, n, m, h). The simulation was done using an Euler scheme with equidistant steps 0.001. Under signal $a = \vartheta = 4$, a deterministic Hodgkin-Huxley neuron (2.1) would be attracted to the stable equilibrium point (2.6). In the stochastic Hodgkin-Huxley neuron (3.2)–(3.4) of Section 3, 'noise' – in the combination of parameters considered here– turns out to be strong enough to create frequent spikes. Here and in all graphics below, no attempt is made towards 'biologically relevant scaling' of the time axis.

In order to feed noise into the system (2.1), we replace adt in the first equation of the deterministic model (2.1) by increments dY_t of a stochastic process

$$Y_t = \vartheta t + X_t \quad , \quad t \geq 0 \tag{3.2}$$

with some constant $\vartheta > 0$, unique strong solution to[3] the stochastic differential equation

$$dY_t = \vartheta(1 + \tau t)dt - \tau Y_t dt + \sigma dW_t. \tag{3.3}$$

Together with equation (3.2) or (3.3), the system

$$\begin{cases} dV_t &= dY_t - F(V_t, n_t, m_t, h_t)dt \\ dn_t &= [\alpha_n(V_t)(1 - n_t) - \beta_n(V_t)n_t]dt \\ dm_t &= [\alpha_m(V_t)(1 - m_t) - \beta_m(V_t)m_t]dt \\ dh_t &= [\alpha_h(V_t)(1 - h_t) - \beta_h(V_t)h_t]dt \end{cases} \tag{3.4}$$

---

[3]SDE (3.3) for the accumulated input $(Y_t)_t$ has remarkable statistical consequences: in the stochastic Hodgkin-Huxley model with constant signal, knowing $\mathbb{X}_0$ and observing the membrane potential V continuously in time, the signal ϑ can be estimated at a better rate than the back-driving force τ ([8], corollary 2 in section 4).

defines a stochastic Hodgkin-Huxley model. We speak of $\vartheta > 0$ as the 'signal' encoded in the system. In contrast to the deterministic case, the behaviour of the biological variables (3.4) in the stochastic system is not only governed by the value of the signal ϑ, but also depends on the level of 'noise', *i.e.* on the values of the volatility σ and the back-driving force τ in the Ornstein-Uhlenbeck process (3.1). We thus consider the 5-dimensional strong Markov process

$$\mathbb{X}^{(\vartheta,\tau,\sigma)} = (\mathbb{X}_t^{(\vartheta,\tau,\sigma)})_{t\geq 0} \quad , \quad \mathbb{X}_t^{(\vartheta,\tau,\sigma)} := (V_t, n_t, m_t, h_t, X_t)_{t\geq 0} \tag{3.5}$$

having state space $E := \mathbb{R} \times [0,1]^3 \times \mathbb{R}$. E is endowed with its Borel-σ-field $\mathcal{E}$. The process (3.5) is homogeneous in time, with encoded signal ϑ and semigroup

$$(P_t^{(\vartheta,\tau,\sigma)})_{t\geq 0}$$

of transition probabilities on $(E, \mathcal{E})$. We suppress superscripts when the context is clear.

A biological interpretation of the system (3.5) is as follows. Assume that the neuron which we consider is part of a large and active network. Then a structure $dY_t = \vartheta dt + dX_t$ of input reflects superposition of some global level $\vartheta > 0$ of excitation in the network with noise in the single neuron. Noise in the single neuron arises as a result of accumulation and decay of a large number of small postsynaptic charges, caused by incoming spikes –registered at synapses, excitatory or inhibitory, present in large number and in complex spatial distribution along the dendritic tree of the neuron, then undergoing decay and finally being summed up– which the neuron receives from a large number of other neurons active within the same network.

Throughout the paper, we exclude by convention unrealistically large values of the signal ϑ: orbits in a deterministic system with same value of the signal always should admit a biological interpretation in terms of a spike. Even if we write '$\vartheta > 0$' below, this is the same caveat as in Section 2.

3.1 Positive Harris recurrence

We discuss ergodicity properties of systems (3.5). For stochastic Hodgkin-Huxley models encoding signals which are deterministic periodic functions, positive Harris recurrence is established in Höpfner, Löcherbach and Thieullen [11, 13], see also [12], and including more general settings in Holbach [7]. Our case of constant signal $\vartheta > 0$ is then essentially a corollary. For background on Harris recurrence see Nummelin [19, 20], Azema, Duflo and Revuz [1], Revuz and Yor [21], Höpfner and Löcherbach [10].

Theorem 3.1. *The following holds for every $\vartheta > 0$, $\tau > 0$, $\sigma > 0$:*

a) *The process $(\mathbb{X}_t^{(\vartheta,\tau,\sigma)})_{t\geq 0}$ is positive Harris recurrent.*

b) *For arbitrary step size $0 < T < \infty$, grid chains $(\mathbb{X}_{kT}^{(\vartheta,\tau,\sigma)})_{k\in\mathbb{N}_0}$ are positive Harris recurrent.*

c) *For arbitrary step size $0 < T < \infty$, chains of path segments*

$$(\mathbb{X}_{[kT,(k+1)T]}^{(\vartheta,\tau,\sigma)})_{k\in\mathbb{N}_0} \quad , \quad \mathbb{X}_{[kT,(k+1)T]}^{(\vartheta,\tau,\sigma)} := (\mathbb{X}_t^{(\vartheta,\tau,\sigma)})_{kT\leq t\leq (k+1)T}$$

with values in the space of continuous functions $C([0,T], E)$ are positive Harris recurrent.

d) *For every $0 < T < \infty$, there is some 'small set' $C \in \mathcal{E}$ of strictly positive invariant measure, some probability law ν on $(E, \mathcal{E})$, and some $\alpha \in (0,1)$ such that Nummelin's minorization condition holds:*

$$P_T^{(\vartheta,\tau,\sigma)}(x, dy) \geq \alpha \mathbb{1}_C(x)\nu(dy) \quad \text{for all } x, y \text{ in } E.$$

Proof. Fix $(\vartheta, \tau, \sigma)$ and write the system (3.5) as

$$\begin{cases} dV_t &=& dX_t - [F - \vartheta](V_t, n_t, m_t, h_t)dt \\ dj_t &=& [\alpha_j(V_t)(1 - j_t) - \beta_j(V_t)j_t]dt \end{cases}, \quad j \in \{n, m, h\}. \tag{3.6}$$

Then (3.6) amounts to a simplified variant of the OU-type Hodgkin-Huxley systems investigated in [11, 13]: we can replace the function F there by $\widetilde{F} := F - \vartheta$, a change which does not affect the proofs in [11] and [13], and then encode $\widetilde{S} \equiv 0$ in place of the deterministic periodic function into the drift of the diffusion process in [11] and [13]. This allows to view any $0 < T < \infty$ as a period for our stochastic system (3.5); the coefficients remain real analytic.

Now a) and b) correspond to Theorems 2.7 and 2.2 in [11]. The lower bound d) corresponds to Theorem 4 and Corollary 1 (together with Sections 6.3 –6.5) in [13], or to step 1) in the proof to Theorem 2.9 in [11]. Assertion c) on path segments follows from b) as in Theorem 2.1 of Höpfner and Kutoyants [9]. □

Let $Q_x^{(\vartheta, \tau, \sigma)}$ denote the law of the process $(\mathbb{X}_t^{(\vartheta, \tau, \sigma)})_{t \geq 0}$ starting from $x \in E$, a probability measure on the canonical path space $(C, \mathcal{C})$ of continuous functions $[0, \infty) \to E$. We equip $(C, \mathcal{C})$ with the right-continuous filtration $\mathbb{G} = (\mathcal{G}_t)_{t \geq 0}$ generated by the canonical process. This allows to view the single neuron $\mathbb{X}^{(\vartheta, \tau, \sigma)}$ in (3.5) as a canonical process on a canonical path space under $Q_x^{(\vartheta, \tau, \sigma)}$. As usual, 'almost surely' means $Q_x^{(\vartheta, \tau, \sigma)}$-almost surely for every $x \in E$.

Positive Harris recurrence Theorem 3.1 a)+b) implies that there exists a unique invariant probability $\mu^{(\vartheta, \tau, \sigma)}$ on the state space $(E, \mathcal{E})$, that sets of positive invariant probability are visited infinitely often (for events $F \in \mathcal{E}$ and arbitrary $0 < T < \infty$,

$$\text{if} \quad \mu^{(\vartheta, \tau, \sigma)}(F) > 0 \quad : \quad \int_0^\infty \mathbb{1}_F(\mathbb{X}_s^{(\vartheta, \tau, \sigma)})ds = \infty \quad , \quad \sum_{k=1}^\infty \mathbb{1}_F(\mathbb{X}_{kT}^{(\vartheta, \tau, \sigma)}) = \infty$$

almost surely), and implies strong laws of large numbers: for functions $h : E \to \mathbb{R}$ which belong to $L^1(\mu^{(\vartheta, \tau, \sigma)})$, limits

$$\frac{1}{t} \int_0^t h(\mathbb{X}_s^{(\vartheta, \tau, \sigma)})ds \longrightarrow \int_E h d\mu^{(\vartheta, \tau, \sigma)} \quad , \quad t \to \infty \tag{3.7}$$

and, for every $0 < T < \infty$ fixed,

$$\frac{1}{n} \sum_{k=1}^n h(\mathbb{X}_{kT}^{(\vartheta, \tau, \sigma)}) \longrightarrow \int_E h d\mu^{(\vartheta, \tau, \sigma)} \quad , \quad n \to \infty \tag{3.8}$$

exist almost surely. Consider also $Q_x^{(\vartheta, \tau, \sigma)}$ restricted to $(C_T, \mathcal{C}_T)$ where C_T is the path space of continuous functions $[0, T] \to \mathbb{R}$, and write

$$Q_\mu^{(\vartheta, \tau, \sigma)} := Q_{\mu^{(\vartheta, \tau, \sigma)}}^{(\vartheta, \tau, \sigma)} = \int_E \mu^{(\vartheta, \tau, \sigma)}(dx) Q_x^{(\vartheta, \tau, \sigma)}$$

for the probability law on $(C, \mathcal{C})$ or on $(C_T, \mathcal{C}_T)$ under which the canonical process $\mathbb{X}$ on $(C, \mathcal{C})$ or on $(C_T, \mathcal{C}_T)$ is a stationary process. If for some T a function $g : C_T \to \mathbb{R}$ belongs to $L^1(Q_\mu^{(\vartheta, \tau, \sigma)})$, then

$$\frac{1}{n} \sum_{k=0}^{n-1} g\left(\mathbb{X}_{[kT, (k+1)T]}^{(\vartheta, \tau, \sigma)}\right) \longrightarrow \int_{C_T} g dQ_\mu^{(\vartheta, \tau, \sigma)} \quad , \quad n \to \infty \tag{3.9}$$

holds almost surely, by positive Harris recurrence Theorem 3.1 c) for path segment chains.

Reinhard Höpfner

3.2 Spike times and spiking patterns

In a stochastic Hodgkin-Huxley neuron (3.5), we define 'beginning' of a spike as the time of upcrossing of the m-variable over the h-variable, and 'end' of the same spike as the time of re-downcrossing of m under h, as in (2.15) in [11]: the membrane potential V reaches its maximum on this time interval almost immediately after the upcrossing of m over h. We define the spike time as the time of the beginning of a spike (the time at which the membrane potential attains a local maximum does not have the structure of a stopping time). Then the spike train emitted by the stochastic Hodgkin-Huxley neuron (3.5) is the sequence $(\tau_j)_{j\geq 1}$ of $\mathbb{G}$-stopping times

$$\tau_j := \inf\{t > \sigma_{j-1} : m_t > h_t\}, \sigma_j := \inf\{t > \tau_j + \delta_0 : m_t < h_t\}, j \geq 1, \sigma_0 = \tau_0 = 0 \quad (3.10)$$

with convention $\inf\{\emptyset\} = \infty$, and with $\delta_0 > 0$ arbitrarily small but fixed. The sequence $(\tau_j)_j$ is strictly increasing and tends to ∞; we associate the counting process

$$N = (N_t)_{t\geq 0} \quad , \quad N_t := \sum_{j\geq 1} \mathbb{1}_{(0,t]}(\tau_j). \quad (3.11)$$

Interspike times $(\tau_j - \tau_{j-1})_{j\geq 1}$ have no reason to be independent or identically distributed, and N has no reason to be a Poisson process (in particular, for every t, the random variable N_t is bounded by construction). This does not exclude the possibility that on compact time intervals, under certain parameter configurations, N with large probability may look quite similar to a Poisson process.

Proposition 3.2.

a) For $0 < T < \infty$ fixed, almost surely within the family of time intervals $\{[kT, (k+1)T] : k \in \mathbb{N}_0\}$, an infinite number of intervals will contain spikes and an infinite number of intervals will remain spikeless.

b) The empirical distribution functions $\widehat{H}_n$ associated to the first n observed interspike times

$$\tau_{\ell+1} - \tau_\ell \quad , \quad 1 \leq \ell \leq n$$

converge almost surely as $n \to \infty$, uniformly on $[0, \infty)$, to the distribution function $H^{(\vartheta,\tau,\sigma)}$ of some probability law which is concentrated on $(0, \infty)$.

Proof. As in the proof of Theorem 3.1, a) and b) correspond to Theorems 2.8 and 2.9 in [11]. □

In the stationary regime, the Laplace transform of the number of spikes observed on path segments of length T

$$\psi_T^{(\vartheta,\tau,\sigma)}(\lambda) := E_\mu^{(\vartheta,\tau,\sigma)}\left(e^{-\lambda N_T}\right) \quad , \quad \lambda \geq 0 \quad (3.12)$$

and the probability that a path segment of length T contains less than v spikes

$$F_T^{(\vartheta,\tau,\sigma)}(v) := Q_\mu^{(\vartheta,\tau,\sigma)}(N_T \leq v) \quad , \quad v \geq 0 \quad (3.13)$$

are of interest for statistical purposes. Whereas there is no hope to get explicit expressions for the left hand sides of (3.12) or (3.13), Harris recurrence provides us with empirical Laplace transforms and empirical distribution functions.

Proposition 3.3. *Under* $(\vartheta, \tau, \sigma)$, *for* $0 < T < \infty$ *fixed,*

a) *the functions*

$$\widehat{\psi}_{n,T}(\lambda) := \frac{1}{n} \sum_{k=1}^{n} e^{-\lambda(N_{kT} - N_{(k-1)T})} \quad , \quad \lambda \geq 0 \quad , \quad n \in \mathbb{N}$$

converge uniformly on $[0, \infty)$, *almost surely as* $n \to \infty$, *to the Laplace transform* $\psi_T^{(\vartheta, \tau, \sigma)}$ *in* (3.12);

b) *the functions*

$$\widehat{F}_{n,T}(v) := \frac{1}{n} \sum_{k=1}^{n} \mathbb{1}_{\{N_{kT} - N_{(k-1)T} \leq v\}} \quad , \quad v \geq 0 \quad , \quad n \in \mathbb{N}$$

converge uniformly on $[0, \infty)$, *almost surely as* $n \to \infty$, *to the distribution function* $F_T^{(\vartheta, \tau, \sigma)}$ *in* (3.13).

Proof. For T, v and λ fixed, both $e^{-\lambda(N_{kT} - N_{(k-1)T})}$ or $\mathbb{1}_{\{N_{kT} - N_{(k-1)T} \leq v\}}$ are bounded functionals $h\left(\mathbb{X}_{[(k-1)T, kT]}\right)$ of paths segments, and pointwise convergence almost surely holds in virtue of Theorem 3.1 c) and (3.9):

$$\frac{1}{n} \sum_{k=1}^{n} h\left(\mathbb{X}_{[(k-1)T, kT]}\right) \longrightarrow E_\mu^{(\vartheta, \tau, \sigma)}\left(h(\mathbb{X}_{[0,T]})\right) \quad , \quad n \to \infty.$$

The limit functions $F_T^{(\vartheta, \tau, \sigma)}$ of (3.13) and $\psi_T^{(\vartheta, \tau, \sigma)}$ of (3.12) are monotonous and bounded, so uniformity on $[0, \infty)$ follows as in the classical proof of the Glivenko-Cantelli Theorem. $\square$

Proposition 3.4. *Under* $(\vartheta, \tau, \sigma)$, *as* $t \to \infty$, *the limit*

$$\lim_{t \to \infty} \frac{1}{t} N_t = E_\mu^{(\vartheta, \tau, \sigma)}(N_1)$$

exists almost surely.

Proof. Fix $T := 1$. View $N_{kT} - N_{(k-1)T}$ as a functional $h\left(\mathbb{X}_{[(k-1)T, kT]}\right)$ of the paths segments; by construction in (3.10), $N_{kT} - N_{(k-1)T}$ being bounded by $\frac{1}{T}\delta_0$, this functional $h : C_T \to [0, \infty)$ is bounded. Theorem 3.1 c) and (3.9) give almost sure convergence

$$\frac{1}{n} N_n = \frac{1}{n} \sum_{k=1}^{n} h\left(\mathbb{X}_{[k-1, k]}\right) \longrightarrow E_\mu^{(\vartheta, \tau, \sigma)}(N_1)$$

under $(\vartheta, \tau, \sigma)$, and with $\lfloor t \rfloor \leq t \leq \lfloor t \rfloor + 1$ the assertion follows. $\square$

The following extension of Proposition 3.2 b) allows to consider spiking patterns.

Theorem 3.5. *For every* $L \in \mathbb{N}$, *empirical distribution functions* $\widehat{G}_m : [0, \infty)^L \to [0, 1]$ *associated to the first* m *observed* L-*tuples of successive interspike times*

$$(\tau_{n+1} - \tau_n, \ldots, \tau_{n+L} - \tau_{n+L-1}), \quad n \in \mathbb{N} \tag{3.14}$$

converge almost surely as $m \to \infty$, *uniformly on* $[0, \infty)^L$, *to the distribution function* $G_\mu^{(\vartheta, \tau, \sigma)}$ *of some probability law concentrated on* $(0, \infty)^L$.

The proof, based on renewal techniques which extend the proof of Proposition 3.2 b) above (*i.e.* the proof of Theorem 2.9 in [11]), is given together with some complements in the appendix Section 7. The probability law $G_\mu^{(\vartheta, \tau, \sigma)}$ in Theorem 3.5 governs the variety of typical patterns on $(0, \infty)^L$ which will appear in the long run in L-tuples of successive interspike times.

3.3 Output of a stochastic Hodgkin-Huxley neuron

The counting process N in (3.11) allows to measure the accumulated activity of the neuron $\mathbb{X}^{(\vartheta,\tau,\sigma)}$ in (3.5) by a stochastic process U which we call 'output'

$$U = (U_t)_{t\geq 0} \quad , \quad dU_t = -c_1 U_{t-}dt + dN_t \quad , \quad U_0 = 0 \tag{3.15}$$

where c_1 is some constant, strictly positive and finite. We have

$$U_t - U_s = U_s e^{-c_1(t-s)} + \int_{(s,t]} e^{-c_1(t-v)}dN_v = U_s e^{-c_1(t-s)} + \sum_{j\geq 1} \mathbb{1}_{(s,t]}(\tau_j)e^{-c_1(t-\tau_j)}$$

for $0 \leq s < t$, and in particular at the spike times

$$U_{\tau_\ell} = \sum_{j=1}^{\ell} e^{-c_1(\tau_\ell - \tau_j)} \quad , \quad U_{\tau_j -} = U_{\tau_{j-1}}e^{-c_1(\tau_j - \tau_{j-1})} \quad , \quad U_{\tau_k} = U_{\tau_k -} + 1. \tag{3.16}$$

Properties of the output process in the long run can be discussed as an application of Theorem 3.5.

Proposition 3.6. *For $\varepsilon > 0$ choose L large enough so that $\sum_{\ell > L} e^{-c_1\delta_0\ell} < \varepsilon$. Then pairs*

$$\left(U_{\tau_{n+L}}, U_{(\tau_{n+L+1})-}\right) \quad , \quad n \in \mathbb{N} \tag{3.17}$$

admit approximations

$$\left(V_n, V_{n+1}^-\right) \quad : \quad V_n := \sum_{j=n}^{n+L} e^{-c_1(\tau_{n+L} - \tau_j)} \quad , \quad V_{n+1}^- := \sum_{j=n}^{n+L} e^{-c_1(\tau_{n+L+1} - \tau_j)} \tag{3.18}$$

with the following properties: we have bounds uniformly in n

$$\sup\left\{|U_{\tau_{n+L}} - V_n|, |U_{(\tau_{n+L+1})-} - V_{n+1}^-| : n \in \mathbb{N}\right\} < \varepsilon,$$

and empirical distribution functions associated to the first m pairs out of (3.18) converge almost surely as $m \to \infty$, uniformly on $[0,\infty)^2$, to the distribution function of some probability law which is concentrated on $(0,\infty)^2$.

The proof of Proposition 3.6 is also shifted to the appendix Section 7. Note that in order to obtain small values of ε in Proposition 3.6 we have to require huge values of L, so the result seems more of theoretical than of practical interest. With the same technique of proof, the result can be extended to $(J+1)$-tuples

$$\left(\left(U_{\tau_{n+j+L}}, U_{(\tau_{n+j+L+1})-}\right)_{0\leq j\leq J}\right), \quad n \in \mathbb{N} \tag{3.19}$$

for $J \in \mathbb{N}$ arbitrary but fixed.

4 Quiet behaviour of stochastic neurons

In a deterministic Hodgkin-Huxley neuron, sufficiently small values of the signal ϑ –smaller than $\inf(\mathbb{I}_{\mathrm{bs}})$, see Section 2– grant that trajectories are attracted to the stable equilibrium point (randomly chosen initial conditions). In a stochastic Hodgkin-Huxley neuron, by Proposition 3.2, spikes will occur almost surely also for small values of the signal ϑ. Simulations under $\vartheta < \inf(\mathbb{I}_{\mathrm{bs}})$ show that the spiking behaviour –in form of single isolated spikes or small groups of spikes– depends on some interplay between the volatility σ and the back-driving force τ.

In Definition 4.1 below, we shall define quiet behaviour of stochastic Hodgkin-Huxley neurons as an event on which spike trains observed over a long time interval seem close
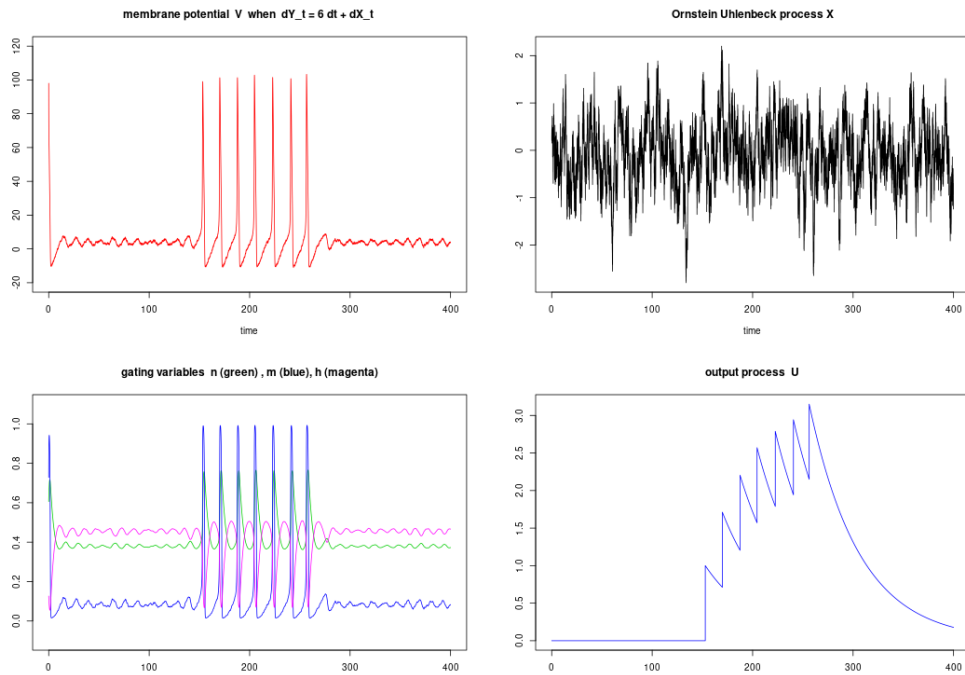
Figure 2: Simulated trajectory of a stochastic Hodgkin-Huxley neuron $\mathbb{X}^{(\vartheta,\tau,\sigma)}$. The signal is $\vartheta = 6$. The parameters for the Ornstein Uhlenbeck process X are $\tau = 0.7$ and $\sigma = 0.83666$. The parameter in the output process U is $c_1 = 0.02$. Initial conditions are selected at random, according to the stationary law of X and according to the uniform law on $(-12, 120) \times (0, 1)^3$ for (V, n, m, h). The starting value for the output process U is 0. The simulation was done using an Euler scheme with equidistant steps 0.001.

to a Poisson process with low intensity. The process N counting spikes has been defined in (3.10).

To random variables $\xi_1, \ldots, \xi_n$, $\mathbb{N}_0$-valued but which in general we do not assume independent or identically distributed, we associate an empirical distribution function $\widehat{F}_n(v) = \frac{1}{n} \sum_{j=1}^n \mathbb{1}_{[0,v]}(\xi_j)$, an empirical Laplace transform $\widehat{\psi}_n(v) := \frac{1}{n} \sum_{j=1}^n e^{-v\xi_j}$, $v \geq 0$, and an empirical mean $\bar{\xi}_n := \frac{1}{n} \sum_{j=1}^n \xi_j$.

For Poisson random variables ξ with parameter $\lambda > 0$, we write $\mathsf{F}_\lambda(v) = \mathsf{P}_\lambda(\xi \leq v)$ for the distribution function (DF), $v \geq 0$, $\phi_\lambda(v) = \mathsf{E}_\lambda(e^{-v\xi})$ for the Laplace transform (LT), and

$$\bar{\mathsf{q}}(\alpha, \lambda) := \min\{n \in \mathbb{N}_0 : \mathsf{P}_\lambda(\xi > n) \leq \alpha\} \tag{4.1}$$

for upper α-quantiles. Write P_λ^n for the joint law of i.i.d. Poisson random variables $(\xi_1, \ldots, \xi_n)$ with parameter $\lambda > 0$, $\widehat{\mathsf{F}}_n$ for the empirical distribution function, $\widehat{\phi_n}$ for the empirical distribution function, and $\bar{\xi}_n$ for the empirical mean. In order to obtain quantified benchmarks for comparison with other data sets we shall use laws

$$\mathcal{L}\left(\int_I \left|\widehat{\mathsf{F}}_n(v) - \mathsf{F}_{\bar{\xi}_n}(v)\right| dv \mid \mathsf{P}_\lambda^n\right) \quad , \quad \mathcal{L}\left(\int_I \left|\widehat{\phi_n}(v) - \phi_{\bar{\xi}_n}(v)\right| dv \mid \mathsf{P}_\lambda^n\right) \tag{4.2}$$

where I is some closed interval in $[0, \infty)$ whose left endpoint is 0, and their upper α-quantiles

$$\bar{\mathsf{q}}_{DF}(\alpha; \lambda, n, I) \quad , \quad \bar{\mathsf{q}}_{LT}(\alpha; \lambda, n, I). \tag{4.3}$$

We shall determine laws (4.2) and quantiles (4.3) empirically using simulations.

On the basis of ergodicity established in Section 3 and motivated in particular by (3.9) and Theorem 3.1 c) applied to path segments of sufficient length T_0, the following definition counts spikes on successive segments

$$\mathbb{X}\mathbb{1}_{](k-1)T_0, kT_0]} \quad , \quad 1 \le k \le K$$

where K is assumed to be large. We call a stochastic Hodgkin-Huxley neuron quiet when i) and ii) hold:

   i) a Poisson-goodness of fit test does not reject a Poisson hypothesis with estimated parameter;

   ii) the estimated parameter is small enough.

Definition 4.1. *Assume that a stochastic Hodgkin-Huxley neuron (3.5) with parameters $(\vartheta, \tau, \sigma)$ has been observed over a long time interval $[0, KT_0]$, $K \in \mathbb{N}$. For K and T_0 large enough, put*

$$T_1 := KT_0 \quad , \quad \widetilde{\lambda} := \frac{1}{T_1} N_{T_1} \quad , \qquad \xi_k := N_{kT_0} - N_{(k-1)T_0} \quad , \quad 1 \le k \le K \qquad (4.4)$$

and fix critical values

$$\lambda_c := 0.0005 \quad , \quad \alpha_c := 0.0005 \qquad (4.5)$$

for hypothetical Poisson intensities and quantiles. Let $Q(T_0, K)$ denote the event in $\mathcal{G}_{T_1}$ on which either: spikes are extremely rare, i.e.

$$N_{T_1} \le 2 \quad and \quad \widetilde{\lambda} \le 0.0001, \qquad (4.6)$$

or: with quantiles (4.1), at most

$$N_{T_1} \le \bar{q}\left(0.05, \lambda_c T_1\right) \qquad (4.7)$$

spikes occur, and their location on the time axis is such that increments $\xi_1, \ldots, \xi_K$ in (4.4) are in good fit with i.i.d. Poisson random variables with estimated parameter $\widetilde{\lambda} T_0$, in the following sense: with $I := [0, 5.5]$ and with $\widehat{F}_K$ and $\widehat{\psi}_K$ defined from $\xi_1, \ldots, \xi_K$ we use the statistics

$$\Delta_{DF}(T_0, K) := \int_I \left| \widehat{F}_K(v) - \mathsf{F}_{\widetilde{\lambda} T_0}(v) \right| dv \quad , \quad \Delta_{LT}(T_0, K) := \int_I \left| \widehat{\psi}_K(v) - \phi_{\widetilde{\lambda} T_0}(v) \right| dv$$

($\mathcal{G}_{T_1}$-measurable) and require, with critical values (4.5) and quantiles (4.3), that the following holds:

$$\Delta_{DF}(T_0, K) \le c_{DF} \quad with \quad c_{DF} := \bar{q}_{DF}\left(\alpha_c; \lambda_c T_0, K, I\right), \qquad (4.8)$$

$$\Delta_{LT}(T_0, K) \le c_{LT} \quad with \quad c_{LT} := \bar{q}_{LT}\left(\alpha_c; \lambda_c T_0, K, I\right). \qquad (4.9)$$

*On events $Q(T_0, K) \in \mathcal{G}_{T_1}$ we call the stochastic neuron $\mathbb{X}$ in (3.5) **quiet**.*

In the setting of Section 3, spike trains are never exactly Poisson (interspike times being $> \delta_0$ by construction, the number N_t of spikes up to time t is bounded by $\frac{1}{\delta_0} t$, for every $t \ge 0$). Under certain parameter configurations, spike trains can however be quite similar to what a Poisson process would show, in particular when very few spikes, all isolated ones, are observed over a long time interval (in contrast to this, see figures 1 and 2). In Definition 4.1, the criterion (4.7) corresponds to a nonrandomized Poisson test for the hypothesis 'unknown intensity is $\le \lambda_c$' versus '$> \lambda_c$' which in a Poisson model would be uniformly most powerful for its level ([23], p. 210), and criteria (4.8) and (4.9) correspond to a Poisson goodness-of-fit test at the critical value λ_c: if N were Poisson with intensity λ_c, the random variables $\Delta_{DF}(T_0, K)$ and $\Delta_{LT}(T_0, K)$ would exceed the critical values in (4.8) and (4.9) in only 5 out of 10^4 cases, on average.

Example 4.2. We use a simulation study to investigate the spiking behaviour of stochastic Hodgkin-Huxley neurons (3.5) with signal $\vartheta = 4$, and to illustrate the influence of the volatility σ and the back-driving force τ in the Ornstein-Uhlenbeck process (3.1) on the spiking behaviour. Recall from Section 2 that under random initial conditions, a deterministic neuron with signal $\vartheta = 4$ would have its trajectories attracted to the stable equilibrium $\left(v^{\{\vartheta\}}, n^{\{\vartheta\}}, m^{\{\vartheta\}}, h^{\{\vartheta\}}\right)$ in (2.6), and trapped there.

Our simulations of trajectories for the stochastic neuron (Euler schemes with time step 0.001) mimick stationary behaviour by omitting, after random initial conditions, a sufficiently long initial piece of trajectory (of length 1000): its terminal state will serve as starting point for a trajectory of total length $T_1 = 25000$, cut down into $K = 100$ segments of length $T_0 = 250$, which we evaluate statistically.

Counting spikes on the $K = 100$ path segments of length $T_0 = 250$ we define as in (4.4)

$$T_1 := KT_0 \quad , \quad \widetilde{\lambda} := \frac{1}{T_1} N_{T_1} \quad , \qquad \xi_k := N_{kT_0} - N_{(k-1)T_0} \quad , \quad 1 \le k \le K$$

and use the criteria and critical values of Definition 4.1. For every parameter configuration $(\vartheta \equiv 4, \tau, \sigma)$ which we consider, we do 10 simulation runs over total time $T_1 = 25000$. This is sufficient to obtain strong evidence – see the tables in 3) below– for the following:

i) the probability $Q_\mu\left(Q(T_0, K)\right) = Q_\mu^{(\vartheta=4, \tau, \sigma)}\left(Q(T_0, K)\right)$ that a simulation run of length T_1 will turn out to be quiet in the sense of Definition 4.1 is a function of τ and σ;

ii) for fixed value of the volatility σ, sufficiently large values of the back-driving force τ (the meaning of 'large' depending on σ) make sure that the neuron will be quiet with probability close to 1.

We explain this in more detail in the following steps 1)–4).

1) With $\lambda_c = 0.0005$ from (4.5), the upper 5%-quantile (4.7) of the Poisson law $\mathsf{P}_{\lambda_c T_1}$ equals

$$\bar{\mathsf{q}}\left(0.05, \lambda_c T_1\right) = 19.$$

With $I = [0, 5.5]$ and $\alpha_c = 0.0005$ as in (4.5), we determine approximate quantiles for criteria (4.8) and (4.9) as follows. To approximate the law under $\mathsf{P}_{\lambda_c T_0}^K$ of the random variables

$$\int_I \left|\widehat{\mathsf{F}}_K(v) - \mathsf{F}_{\bar{\xi}_K}(v)\right| dv \quad , \quad \int_I \left|\widehat{\phi}_K(v) - \phi_{\bar{\xi}_K}(v)\right| dv \tag{4.10}$$

we draw i.i.d. Poisson random variables $\xi_1, \ldots, \xi_K$ with parameter $\lambda_c T_0$ and calculate the integrals (4.10) for these. After a large number of $4 \cdot 10^4$ replications, empirical distribution functions for the objects in (4.10) are sufficiently good to determine upper α_c-quantiles approximately:

$$\bar{\mathsf{q}}_{DF}(\alpha_c; \lambda_c T_0, K, I) \approx 0.075 \quad , \quad \bar{\mathsf{q}}_{LT}(\alpha_c; \lambda_c T_0, K, I) \approx 0.15. \tag{4.11}$$

Approximations (4.11) yield critical values c_{DF} and c_{LT} for conditions (4.8) and (4.9).

2) In every simulation run, with $\xi_1, \ldots, \xi_K$ and $\widetilde{\lambda}$ given by (4.4), we have

$$\widetilde{\lambda} T_0 = \frac{N_{T_1}}{T_1} T_0 = \frac{1}{K} N_{T_1} = \frac{1}{K} \sum_{j=1}^K \xi_j = \bar{\xi}_K$$

and calculate from $\xi_1, \ldots, \xi_K$ the integrals

$$\Delta_{DF}(T_0, K) := \int_I \left|\widehat{F}_K(v) - \mathsf{F}_{\widetilde{\lambda} T_0}(v)\right| dv \quad , \quad \Delta_{LT}(T_0, K) := \int_I \left|\widehat{\psi}_K(v) - \phi_{\widetilde{\lambda} T_0}(v)\right| dv.$$

We check conditions (4.8) and (4.9) in combination with either (4.6) or (4.7). When the full set of conditions is satisfied, the simulation run is counted as quiet in the sense of Definition 4.1. We repeat 10 runs under every parameter configuration which we consider.

3) With signal $\vartheta = 4$, we vary the volatility σ and the back-driving force τ. As a general feature, when σ is fixed, spikes turn out to be rare under 'large' values of τ whereas they are frequent under 'low' values of τ (figure 1 provides an illustration for the last case). In 3i)–3iii) below, we report in more detail the outcome of the simulation study for selected values of σ and τ.

i) For signal $\vartheta = 4$ and volatility $\sigma = 2.5$, interesting τ-values range between 2.0 and 2.4. Figure 3 shows empirical distribution functions for the random variables N_{T_1}, $\Delta_{DF}(T_0, K)$ and $\Delta_{LT}(T_0, K)$ obtained from the 10 simulation runs. Vertical dotted lines indicate the critical values in (4.7), (4.8) and (4.9) as specified in 1). The following percentages of runs turned out to be quiet in the sense of Definition 4.1:

$\tau = 2.0$	$\tau = 2.1$	$\tau = 2.2$	$\tau = 2.3$	$\tau = 2.4$
0%	10%	60%	100%	100%

Among runs which did not fulfill all requirements of Definition 4.1, some failed with respect to Poisson-goodness of fit (4.8) or (4.9) while satisfying (4.7), and some runs failed to (4.7) while satisfying (4.8) and (4.9). Figure 3 provides evidence that for ϑ and σ fixed, laws of N_{T_1}, $\Delta_{DF}(T_0, K)$ and $\Delta_{LT}(T_0, K)$ do depend on τ. Figure 3 suggests in addition that laws under $Q_\mu^{(\vartheta, \tau, \sigma)}$ of these three variables should be stochastically ordered in τ, in the sense that larger values of the back-driving force tend (while reducing among all observed spikes the proportion of double or triple ones) to reduce the total number of spikes and to improve the quality of Poisson approximation. As an example, the 10 simulation runs (over total time $T_1 = 25000$) produced in average 37.4 spikes under $\tau = 2.0$, in contrast to 5.6 in average under $\tau = 2.4$.

ii) For signal $\vartheta = 4$ and volatility $\sigma = 1.5$, results of similar structure as described in 3i) were observed, but now the interesting range of τ-values is between 1.0 and 1.4. In the 10 simulation runs, the following percentage turned out to be quiet in the sense of Definition 4.1:

$\tau = 1.0$	$\tau = 1.1$	$\tau = 1.15$	$\tau = 1.2$	$\tau = 1.3$	$\tau = 1.4$
0%	0%	30%	70%	80%	100%

The empirical distribution functions in figure 4 illustrate the dependence of the laws of all three variables N_{T_1}, $\Delta_{DF}(T_0, K)$ and $\Delta_{LT}(T_0, K)$ on the back-driving force τ, and provide a strong hint that laws under $Q_\mu^{(\vartheta, \tau, \sigma)}$ of the three variables should be stochastically ordered in the sense of decreasing values of τ. Most striking example, the 10 simulation runs (with $T_1 = 25000$) produced an average of 51.1 spikes under $\tau = 1.0$, in strong contrast to an average of only 2.5 under $\tau = 1.4$.

iii) For signal $\vartheta = 4$ and volatility $\sigma = 1.0$, we observe the same features as in 3i) and 3ii). The interesting range of τ-values is now between 0.5 (frequent spikes) and 0.75 (few spikes), and the following percentages of runs turned out to be quiet in the sense of Definition 4.1:

$\tau = 0.5$	$\tau = 0.55$	$\tau = 0.6$	$\tau = 0.65$	$\tau = 0.7$	$\tau = 0.75$
0%	20%	50%	90%	100%	100%

4) We sum up as follows: when the signal is $\vartheta = 4$, the schemes in 3i)–3iii) above prove the dependence of $Q_\mu^{(\vartheta,\tau,\sigma)}\left(Q(T_0, K)\right)$ on the volatility $\sigma > 0$ and the back-driving force $\tau > 0$. Stronger values of τ tend to reduce the total number of spikes and to improve the quality of Poisson approximation. For actual determination of probabilities of events $Q(T_0, K) \in \mathcal{G}_{T_1}$ in stationary regime, we would of course need much more than the 10 simulation runs (up to time $T_1 = 25000$, under every parameter configuration) which we have done. So the above tables above can give only poor approximations so far.
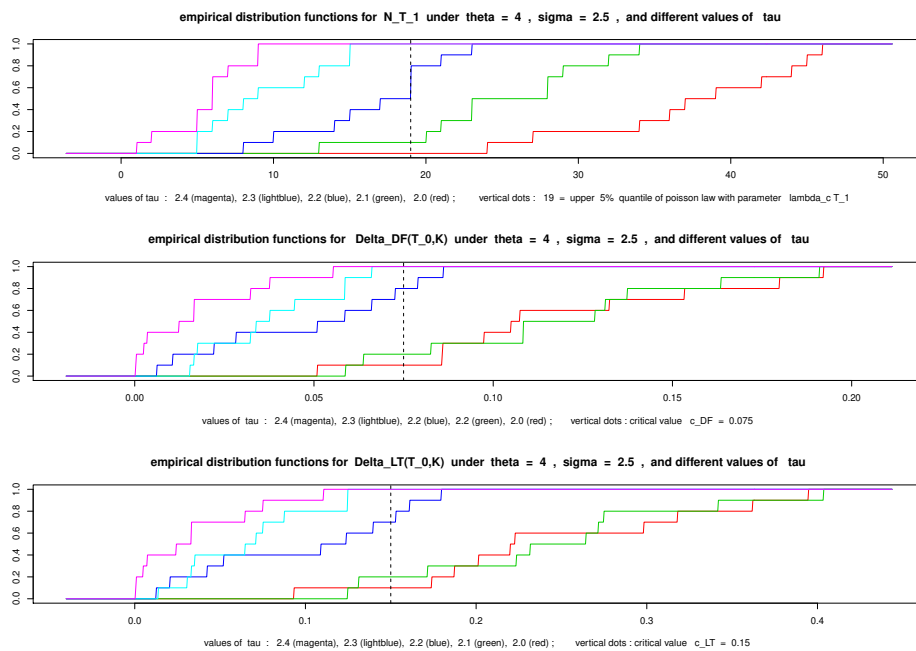

empirical distribution functions for N_T_1 under theta = 4 , sigma = 2.5 , and different values of tau

values of tau : 2.4 (magenta), 2.3 (lightblue), 2.2 (blue), 2.1 (green), 2.0 (red) ;   vertical dots : 19 = upper 5% quantile of poisson law with parameter lambda_c T_1

empirical distribution functions for Delta_DF(T_0,K) under theta = 4 , sigma = 2.5 , and different values of tau

values of tau : 2.4 (magenta), 2.3 (lightblue), 2.2 (blue), 2.2 (green), 2.0 (red) ;   vertical dots : critical value c_DF = 0.075

empirical distribution functions for Delta_LT(T_0,K) under theta = 4 , sigma = 2.5 , and different values of tau

values of tau : 2.4 (magenta), 2.3 (lightblue), 2.2 (blue), 2.1 (green), 2.0 (red) ;   vertical dots : critical value c_LT = 0.15

Figure 3: In the stochastic Hodgkin-Huxley model with signal $\vartheta = 4$, volatility $\sigma = 2.5$, and values of the back-driving force τ varying between 2.0 and 2.4, we show empirical distribution functions for the laws of the random variables N_{T_1}, $\Delta_{DF}(T_0, K)$, $\Delta_{LT}(T_0, K)$ under $(\vartheta, \sigma, \tau)$. These are based on the values which have been observed in the 10 simulation runs described in 3i) of example 4.2, on a time interval of length $T_1 = 25000$ divided into $K = 100$ segments of length $T_0 = 250$. The graphics suggest stochastic ordering of the laws under $Q_\mu^{(\vartheta,\tau,\sigma)}$ for all three variables, most clearly visible in case of the total number N_{T_1} of spikes, in the sense of decreasing values of τ.

5 Regular spiking of stochastic neurons

In deterministic Hodgkin-Huxley neurons, regular spiking –in the sense that trajectories are attracted towards a stable orbit– depends only on the value of the signal ϑ: with notations of Section 2, this is the case $\vartheta > \sup(\mathbb{I}_{bs})$ where we exclude, as in Section 2, unrealistically large values of the signal.

For a stochastic Hodgkin-Huxley neuron, given Proposition 3.2 or Theorem 3.5, we shall define regular spiking as an event where up to some sufficiently large time T_1, the pattern of observed spike times is sufficiently close to a regularly spaced grid whose
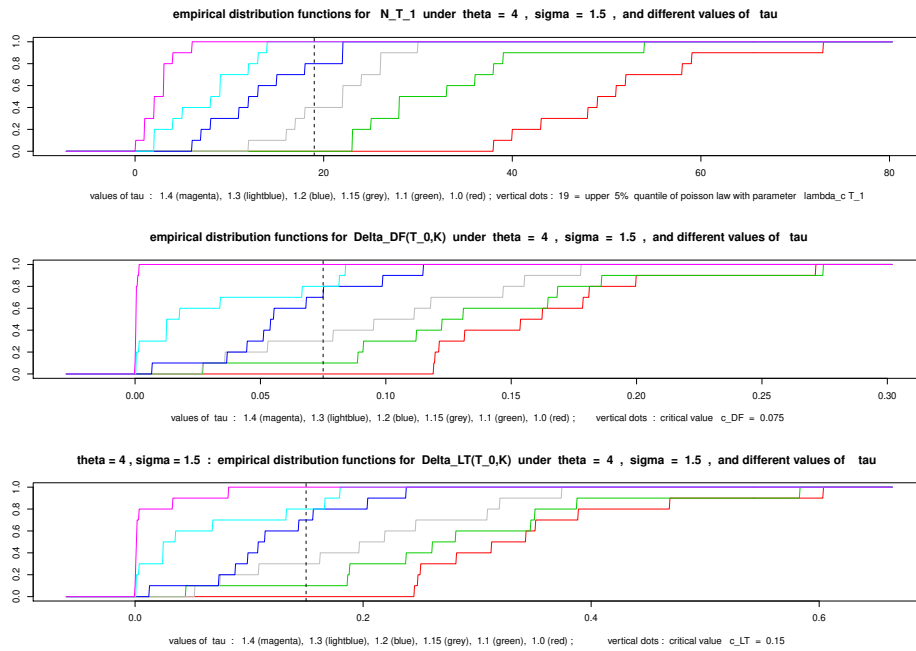
empirical distribution functions for N_T_1 under theta = 4 , sigma = 1.5 , and different values of tau

values of tau : 1.4 (magenta), 1.3 (lightblue), 1.2 (blue), 1.15 (grey), 1.1 (green), 1.0 (red) ; vertical dots : 19 = upper 5% quantile of poisson law with parameter lambda_c T_1

empirical distribution functions for Delta_DF(T_0,K) under theta = 4 , sigma = 1.5 , and different values of tau

values of tau : 1.4 (magenta), 1.3 (lightblue), 1.2 (blue), 1.15 (grey), 1.1 (green), 1.0 (red) ;   vertical dots : critical value c_DF = 0.075

theta = 4 , sigma = 1.5 : empirical distribution functions for Delta_LT(T_0,K) under theta = 4 , sigma = 1.5 , and different values of tau

values of tau : 1.4 (magenta), 1.3 (lightblue), 1.2 (blue), 1.15 (grey), 1.1 (green), 1.0 (red) ;   vertical dots : critical value c_LT = 0.15

Figure 4: In the stochastic Hodgkin-Huxley model with signal $\vartheta = 4$, volatility $\sigma = 1.5$, and values of the back-driving force τ varying between 1.0 and 1.4, we show empirical distribution functions for the laws of the random variables N_{T_1}, $\Delta_{DF}(T_0, K)$, $\Delta_{LT}(T_0, K)$ under $(\vartheta, \tau, \sigma)$. They are based on the values which have been observed in the 10 simulation runs described in 3ii) of Example 4.2, on a time interval of length $T_1 = 25000$ divided into $K = 100$ segments of length $T_0 = 250$. The graphics suggest strongly that laws under $Q_\mu^{(\vartheta, \tau, \sigma)}$ for all three variables should be stochastically ordered in the sense of decreasing values of τ.

step size is the median

$$\Delta(T_1) := \text{median} \left(\tau_2 - \tau_1, \ldots, \tau_{N_{T_1}} - \tau_{N_{T_1}-1} \right) \tag{5.1}$$

of the interspike times. Simulations indicate that the probability of such events in $\mathcal{G}_{T_1}$ in stationary regime depends on the triplet of parameters $(\vartheta, \tau, \sigma)$: for signal $\vartheta > \sup(\mathbb{I}_{bs})$, we can expect regular spiking in the sense of Definition 5.1 with probability close to 1 whenever back-driving force τ in the Ornstein-Uhlenbeck process (3.1) is –in relation to the value σ of the volatility– large enough.

Fix $T_1 < \infty$ and assume that a sufficiently large number of interspike times

$$\tau_2 - \tau_1, \ldots, \tau_{N_{T_1}} - \tau_{N_{T_1}-1} \tag{5.2}$$

has been observed up to time T_1. Write $\widehat{H}_{T_1}$ for the empirical distribution function of the data set (5.2). Write

$$\Delta(T_1) = \inf\{v > 0 : \widehat{H}_{T_1}(v) \geq 0.5\}$$

for the median and

$$\mathrm{d}(\alpha, T_1) := \inf\{v > 0 : \widehat{H}_{T_1}(v) \geq 1 - \alpha\} - \inf\{v > 0 : \widehat{H}_{T_1}(v) \geq \alpha\}$$

for the distance between upper and lower α-quantiles in the data set (5.2), $0 < \alpha < \frac{1}{2}$; relating quantile distances to the median we shall consider ratios

$$\mathtt{r}(\alpha, T_1) := \frac{\mathtt{d}(\alpha, T_1)}{\Delta(T_1)}. \tag{5.3}$$

The next Definition builds on weak convergence of empirical distributions for the interspike times, as time goes to infinity, in application of Proposition 3.2: in the long run under $(\vartheta, \tau, \sigma)$, 'typical' interspike times are distributed according to $H^{(\vartheta, \tau, \sigma)}$. If we have no grasp on the limiting object itself, presence of noise in the system (3.4) –as illustrated by figures such as 1, 2 or 6 or by detailed representations of the system evolving on 'orbits' – strongly suggests that $H^{(\vartheta, \tau, \sigma)}$ in Proposition 3.2 b) has to be strictly increasing and continuous on some interval of support. In fact, flats in the limit distribution function seem impossible under noise –this would imply existence of pairs $0 < x_1 < x_2 < \infty$ with $0 < H^{(\vartheta, \tau, \sigma)}(x_1) = H^{(\vartheta, \tau, \sigma)}(x_2) < 1$ and thus non-existence of interspike times of length between x_1 and x_2 in the long run under $(\vartheta, \tau, \sigma)$– as well as point masses. But then, arbitrary quantiles of the empirical distribution functions ([24] p. 71, without exceptional set) should converge to those of the limit distribution function, as a consequence of Proposition 3.2 b) . See also Proposition 8.3 in the Appendix Section 8.

Definition 5.1. *Consider a stochastic Hodgkin-Huxley neuron* (3.5) *under* $(\vartheta, \tau, \sigma)$. *With notations* (5.1)–(5.3) *and for* T_1 *large enough, define* $R(T_1)$ *as the event in* $\mathcal{G}_{T_1}$ *on which*

$$\left| \frac{N_{T_1} \Delta(T_1)}{T_1} - 1 \right| \leq 0.05 \quad \text{and} \quad N_{T_1} > 20 \tag{5.4}$$

holds together with

$$\mathtt{r}(0.05, T_1) \leq 0.3, \quad \mathtt{r}(0.1, T_1) \leq 0.2, \quad \mathtt{r}(0.25, T_1) \leq 0.1. \tag{5.5}$$

On the event $R(T_1) \in \mathcal{G}_{T_1}$ *we call the stochastic neuron* $\mathbb{X}$ **regularly spiking**.

Condition (5.5) requires that quantiles in the data set (5.2) of interspike times are close to the median, but does not rule out (as illustrated by Figure 2) that up to time T_1, few long spikeless periods alternate with long groups of regularly spaced spikes. This is why (5.4) requires regular spacing on at least 95% of the time interval on which the membrane potential is observed.

Example 5.2. As in classical statistics of i.i.d. observations, we can approximate $Q_\mu^{(\vartheta, \tau, \sigma)}(R(T_1))$ from independent replications of $\mathbb{X}^{(\vartheta, \sigma, \tau)}$ in stationary regime over time intervals of length T_1. We consider signal $\vartheta = 10$ (for which the deterministic process would evolve along a stable orbit, see section 2) together with different values of τ and σ.

We use Euler schemes of step size 0.001. In order to mimick stationary regime, in every simulation run, we cast away an initial piece of trajectory (of length 100) under randomly chosen initial conditions (uniformly on $(-12, 120) \times (0, 1)^3$ for (V, n, m, h) and according to the stationary law for X; the output U starts at 0), conserve the final state of this initial piece of trajectory as starting point for the simulation of interest which then covers a time interval of length $T_1 = 500$. This second piece of trajectory is used for inference.

Thus, for $\vartheta = 10$ and $T_1 = 500$, we simulate 20 runs under every parameter configuration. The scheme below gives the proportion of runs where regular spiking in the sense of Definition 5.1 was observed.

	$\tau = 0.1$	$\tau = 0.5$	$\tau = 1$	$\tau = 2.5$	$\tau = 5$
$\sigma = 1$	100%	100%	100%	*100%	*100%
$\sigma = 1.5$	55%	90%	100%	100%	*100%
$\sigma = 2.5$	15%	45%	75%	100%	100%
$\sigma = 5$	0%	5%	20%	95%	100%

We deduce that in stationary regime, the event $R(T_1) \in \mathcal{G}(T_1)$ has probability close to 1 for well-chosen pairs (τ, σ): either, depending on σ, the back-driving force τ has to be strong enough, or, depending on τ, the volatility σ has to be small enough. Asterisk * distinguishes parameter configurations under which observed ratios $\mathbf{r}(0.05, T_1)$ in (5.5) turned out –on average over the 20 simulation runs– to be strictly smaller than 0.05, whereas the median $\Delta(T_1)$ was located between 14.3 and 14.4. In this sense, an upper right triangle of parameter values shows up in the scheme where quantiles of the data set (5.2) concentrate sharply at the median, and empirical distribution functions for the observed values of

$$\mathbf{r}(0.05, T_1) \quad , \quad \mathbf{r}(0.1, T_1) \quad , \quad \mathbf{r}(0.25, T_1) \tag{5.6}$$

in the 20 simulation runs under $\vartheta = 10$ (not shown) look very much as a Dirac mass at $\Delta(T_1)$ under 'some small random perturbation'. Figure 5 below shows empirical distribution functions for observed values of ratios (5.6) in case of rather high volatility $\sigma = 2.5$ for all values $\tau \in \{0.1, 0.5, 1.0, 2.5, 5.0\}$ in the scheme under $\vartheta = 10$. The graphics indicate that in stationary regime, laws of variables (5.6) seem to be stochastically ordered in the back-driving force τ, in the sense that increasing values of τ tend to push quantiles $\mathbf{q}(\alpha, T_1)$ closer to the median $\Delta(T_1)$.

By (3.15)–(3.16), the output U of a stochastic Hodgkin-Huxley neuron (3.5) fluctuates between 'typical values' of U_{τ_ℓ} (local maxima) and $U_{(\tau_{\ell+1})^-} = U_{\tau_\ell} e^{-c_1(\tau_{\ell+1} - \tau_\ell)}$ (local minima) as $\ell \to \infty$. In general, typical values refers to the approximations and limit distributions of Proposition 3.6. If however the neuron is regularly spiking, 'typical values' takes a much sharper sense: simulations suggest that on events $R(T_1)$ as defined in 5.1, for T_1 large enough, functions of $\Delta(T_1)$

$$\sum_{j \geq 0} e^{-c_1 \Delta(T_1) j} = \frac{1}{1 - e^{-c_1 \Delta(T_1)}} \quad , \quad \sum_{j \geq 0} e^{-c_1 \Delta(T_1)(j+1)} = \frac{e^{-c_1 \Delta(T_1)}}{1 - e^{-c_1 \Delta(T_1)}} \tag{5.7}$$

provide benchmarks which allow to predict where pairs U_{τ_ℓ}, $U_{(\tau_{\ell+1})^-}$ tend to cluster in the long run, hence predict an interval on which the output process tends to concentrate a predominant part of future occupation time. Figure 6 provides an illustration.

We shall discuss in an appendix section 8 in which sense (5.7) is expected to provide good approximations to future values of the output process, on events $R(T_1)$ when T_1 is large.

In numerous simulations with large values of signal ϑ and large observation time T_1, whenever the stochastic neuron turned out to be regularly spiking in the sense of Definition 5.1, benchmarks (5.7) predicted well the range of oscillations of the output process once time was large enough.

6 Circuits of stochastic Hodgkin-Huxley neurons

This section describes circuits of interacting stochastic Hodgkin-Huxley neurons where activity shows up in form of blocks of spiking neurons performing slow and rhythmic oscillation around the circuit. This self-organized rhythmic behaviour of activity patterns seems to be persistent in the long run. We are however unable to prove persistence –however strongly suggested by simulations– and restrict this section to a detailed description of the construction and to some motivating remarks. Our construction relies on the notions of 'quiet behaviour' (Definition 4.1) and of 'regular spiking' (Definition 5.1)in order to define the interactions between the neurons in the circuit.

It seems admitted that in networks of biological neurons [15, 5], information transfer happens in form of excitation and inhibition at a large number of synapses, a by far
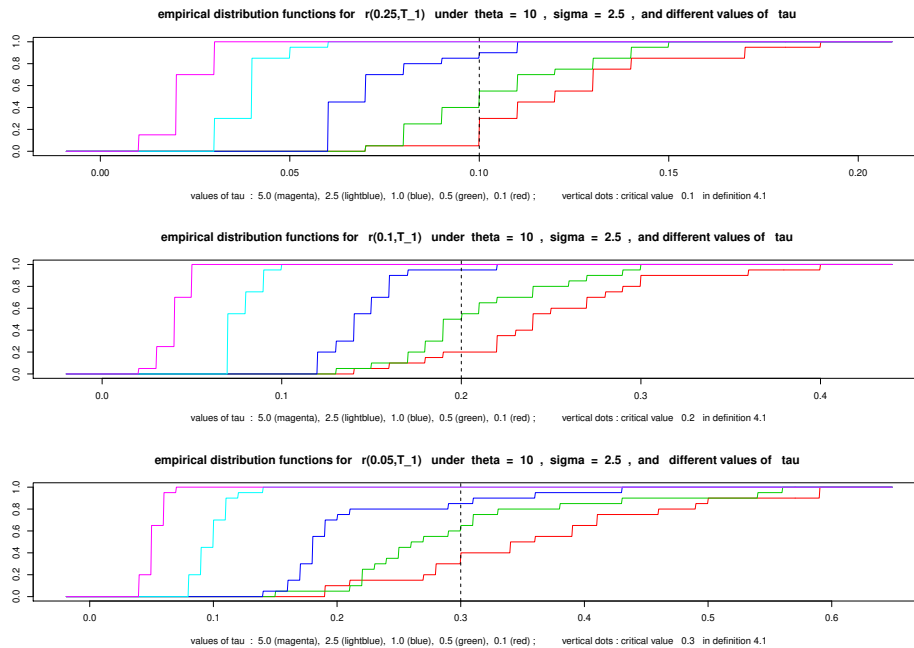
Figure 5: In the stochastic Hodgkin-Huxley model with signal $\vartheta = 10$, volatility $\sigma = 2.5$, and values of the back-driving force τ varying between 0.1 and 5.0, we show empirical distribution functions for the laws of the random variables $\mathtt{r}(0.25, T_1)$, $\mathtt{r}(0.1, T_1)$, $\mathtt{r}(0.05, T_1)$ under $(\vartheta, \sigma, \tau)$, in stationary regime and with $T_1 = 500$. The empirical distribution functions are based on the values which have been observed in the 20 simulation runs described in Example 5.2. The graphics suggest that laws of all three random variables under $Q_\mu^{(\vartheta, \tau, \sigma)}$ should be stochastically ordered in τ, in the sense that increasing values of τ improve remarkably the concentration of interspike times around their median. The median $\Delta(T_1)$ itself (as well as the number of spikes in the observation interval) does not change much with τ: averaged over the 20 runs we obtained 14.19 for $\tau = 0.1$, and 14.33 for $\tau = 5.0$.

larger part of the synapses in the network being excitatory. In our circuit of interacting stochastic Hodgkin-Huxley neurons, we impose a block structure of the following type: information transfer from one neuron to the next along the circuit will be excitatory as long as we remain inside the same block, and will be inhibitory when we pass from the last neuron in a block to the first neuron in its successor block. In this block-wise construction of the circuit, as a consequence of excitation and inhibition, self-organized patterns of oscillation show up quite rapidly. Spiking activity is propagating from block to block around the circuit: while some blocks are regularly spiking and in this sense active, others are quiet at the same time, and at certain times, blocks flip from active to quiet, and back from quiet to active. In this way, block-wise activity patterns arise and perform a slow rotation along the circuit. This rotational movement seems to be persistent. However, nothing being proved so far, we only give the construction.

Modelization Step 6.1 (Selecting suitable parameter values). With reference to the bistability interval $\mathbb{I}_{\mathrm{bs}}$ of the deterministic case in Section 2, we fix parameter values

$$0 < \vartheta_1 := \lfloor \inf(\mathbb{I}_{\mathrm{bs}}) - 1 \rfloor, \quad \vartheta_2 := \lceil \sup(\mathbb{I}_{\mathrm{bs}}) + 1 \rceil, \quad 0 < \tau < \infty \quad , \quad 0 < \sigma < \infty \qquad (6.1)$$
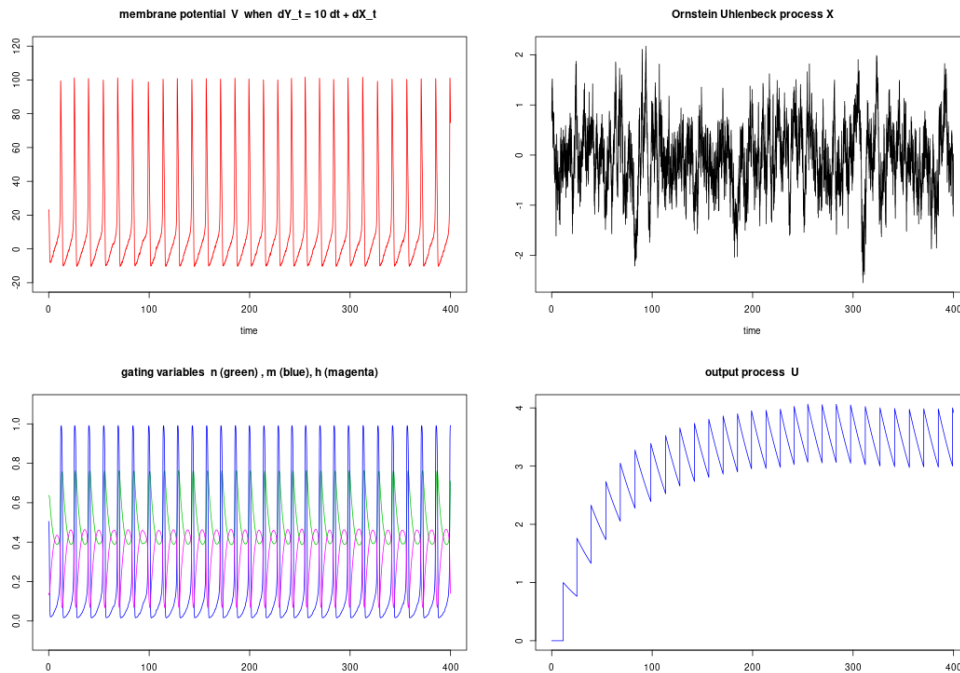
Figure 6: Simulated trajectory of a stochastic Hodgkin-Huxley neuron $\mathbb{X}^{(\vartheta,\tau,\sigma)}$. The signal is $\vartheta = 10$. The parameters for the OU process X are $\tau = 0.7$ and $\sigma = 0.83666$. The decay parameter in the output process U is $c_1 = 0.02$. The simulation was done using an Euler scheme with equidistant steps 0.001. We start with $U_0 = 0$ and random initial conditions for (V, n, m, h, X). In this simulation, 27 spikes occur up to time $T_1 = 400$. The median of the 26 interspike times is $\Delta(T_1) = 14.4$, lower resp. upper 25%-quantiles are at 14.07 resp. 14.69, the minimum is 13.87 and the maximum 15.23. Longer and shorter interspike times seem to alternate at random. Benchmarks (5.7) take the value 3.99 for local maxima of the output process in the long run, and 2.99 for local minima. The interval $(2.99, 3.99)$ is in good fit with the range of oscillations of the output process U on the second half of the time interval of observation.

such that a single stochastic Hodgkin-Huxley neuron (3.5) in stationary regime tends to be

quiet under $(\vartheta_1, \tau, \sigma)$ in the sense of Definition 4.1 ,

regularly spiking under $(\vartheta_2, \tau, \sigma)$ in the sense of Definition 5.1,

where we require that the back-driving force τ and the volatility σ be the same in both cases.

Our choices in modelization step 6.1 require more explanation. First, in stationary regime and for T_0 and K sufficiently large in the sense of Definition 4.1 and Example 4.2, we have to identify pairs (τ, σ) such that the probability to find the single stochastic Hodgkin-Huxley neuron (3.5) under $(\vartheta_1, \tau, \sigma)$ in the event $Q(T_0, K) \in \mathcal{G}_{T_1}$ is close to 1. Second, in stationary regime and for T_1 as in Definition 5.1 and Example 5.2 (which represents a different choice of T_1), we have to identify pairs (τ, σ) such that the probability to find a single stochastic Hodgkin-Huxley neuron (3.5) under $(\vartheta_2, \tau, \sigma)$ in the event $R(T_1) \in \mathcal{G}_{T_1}$ is close to 1. Third, we have to select **one** pair (τ, σ) which meets both requirements. This is possible.

Example 6.2. As an example, with values

$$\vartheta_1 = 4 \quad , \quad \vartheta_2 = 10 \tag{6.2}$$

satisfying (6.1) according to the numerical considerations of Section 2, the simulations in Examples 4.2 and 5.2 indicate that a combination of the volatility and the back-driving force of the form

$$\sigma = 1.0 \quad \text{and} \quad \tau \geq 0.7 \quad , \quad \sigma = 1.5 \quad \text{and} \quad \tau \geq 1.4 \quad , \quad \sigma = 2.5 \quad \text{and} \quad \tau \geq 2.5$$

meet the requirements of modelization step 6.1. See the schemes in step 3) of 4.2, and the scheme in Example 5.2.

For the stochastic neuron under $(\vartheta_2, \tau, \sigma)$ –regularly spiking with probability close to 1 up to time T_1– we fix a prediction $\Delta^* = \Delta^*(\vartheta_2, \tau, \sigma)$ for the median of interspike times in stationary regime in the long run: combining modelization step 6.1 and Example 5.2, with T_1, $R(T_1)$, $\Delta(T_1)$ from Example 5.2, we define

$$\Delta^* := \Delta(T_1) \tag{6.3}$$

which is the median of the interspike times observed up to time T_1. Every choice of a decay parameter c_1 in view of a construction (3.15) of an output process U then associates to Δ^* an interval (5.7)

$$(u_1^*, u_2^*) \quad , \quad u_2^* := \sum_{j=0}^{\infty} e^{-c_1 j \Delta^*} \quad , \quad u_1^* := \sum_{j=0}^{\infty} e^{-c_1(j+1)\Delta^*} \tag{6.4}$$

on which we expect the output process U to accumulate a large amount of occupation time in the long run. We wish to scale the shape of output processes for regularly spiking neurons more or less independently of the parameters $(\vartheta_2, \tau, \sigma)$ and thus of Δ^*.

Modelization Step 6.3 (Calibration of the decay parameter for output processes)**.** From Δ^* in (6.3) define

$$c^* := -\log\left(\frac{3}{4}\right) / \Delta^*;$$

then, by an 'adapted' choice of the decay parameter $c_1 > 0$ in (3.15) , we consider intervals (6.4) which approximately do not depend on the parameters:

$$c_1 \approx c^* \quad , \quad u_2^* = (1 - e^{-c_1 \Delta^*})^{-1} \approx (1 - e^{-c^* \Delta^*})^{-1} = 4 \quad , \quad u_1^* \approx 3. \tag{6.5}$$

Modelization Step 6.4 (Choice of transmission functions)**.** Select some smooth and strictly increasing function $\Psi^* : \mathbb{R} \to [0, 1]$ with the properties

$$\lim_{v \to -\infty} \Psi^*(v) = 0 \quad , \quad \Psi^*(1) < 0.025 \quad , \quad \Psi^*(u_1^*) > 0.975 \quad , \quad \lim_{v \to \infty} \Psi^*(v) = 1 \tag{6.6}$$

for c_1 and (u_1^*, u_2^*) selected in (6.5). For $\vartheta_1 < \vartheta_2$ determined in modelization step 6.1, use Ψ^* to define a pair of transmission functions

$$\begin{cases} \Psi_{\mathrm{exc}}(x) & := & \vartheta_1 + (\vartheta_2 - \vartheta_1)\Psi^*(x) \\ \Psi_{\mathrm{inh}}(x) & := & \vartheta_2 - (\vartheta_2 - \vartheta_1)\Psi^*(x) \end{cases} \quad , \quad x \in \mathbb{R}. \tag{6.7}$$

The first function in (6.7) will be used to model excitation, the second inhibition.

As an example, using well known properties of the standard normal distribution function Φ and its quantiles, a choice

$$\Psi^*(x) := \Phi\left(\frac{x - \frac{1+u_1^*}{2}}{\frac{u_1^*-1}{6}}\right)$$

will satisfy (6.6). The transmission functions in (6.7), excitatory or inhibitory, serve as a key tool to model information transfer between neurons in the circuit under construction.

Modelization Step 6.5 (Construction of the circuit). Fix an integer $M \geq 3$ which is odd, and some integer $L \geq 4$. We shall construct a circuit of $N := ML$ neurons

$$\mathcal{N}^{(1)}, \ldots, \mathcal{N}^{(N)} \tag{6.8}$$

where we count neurons around the circuit modulo N: in particular, $\mathcal{N}^{(0)}$ and $\mathcal{N}^{(N)}$ are different names for the same neuron in the circuit, $\mathcal{N}^{(N+1)}$ is $\mathcal{N}^{(1)}$, and so on. We arrange neurons along the circuit (6.8) in M blocks

$$\{1, \ldots, L\}, \{L+1, \ldots, 2L\}, \ldots, \{(M-1)L+1, \ldots, N\} \tag{6.9}$$

each of which contains L neurons. Subsets of indices

$$I_{\text{inh}} := \{1, L+1, \ldots, (M-1)L+1\} \quad , \quad I_{\text{exc}} := \{1, \ldots, N\} \setminus I_{\text{inh}} \tag{6.10}$$

will be used to distinguish neurons $i \in I_{\text{inh}}$ which occupy the first position in their block (i.e.: i equals 1 modulo L) from neurons $i \in I_{\text{exc}}$ which have their predecessor in the same block. We emphasize that the number M of blocks in (6.9) has to be **odd**.

In the circuit (6.8) with its block structure (6.9)–(6.10) –where the successor of neuron $\mathcal{N}^{(N)}$ is $\mathcal{N}^{(1)}$ and the predecessor of neuron $\mathcal{N}^{(1)}$ is $\mathcal{N}^{(N)}$, in the sense of the circuit– neurons $\mathcal{N}^{(i)}$, $i \in I_{\text{exc}}$, will be excited by their predecessor, and neurons $\mathcal{N}^{(i)}$, $i \in I_{\text{inh}}$, will be inhibited by their predecessor. So transfer inside blocks will always be excitatory; from the last neuron in a block to the first neuron in the following block, transfer will be inhibitory.

a) For the pair (τ, σ) which has been selected in modelization step 6.1, prepare $N = ML$ independent Ornstein-Uhlenbeck processes $X^{(i)}$, strong solutions to equations

$$dX_t^{(i)} = -\tau X_t^{(i)}dt + \sigma dW_t^{(i)} \quad , \quad 1 \leq i \leq N$$

driven by independent Brownian motions $W^{(i)}$. We stress that by choice in modelization step 6.1, the back-driving force and the volatility are the same for all processes $X^{(i)}$, $1 \leq i \leq N$.

b) With stochastic processes $A^{(i)} = (A_t^{(i)})_{t \geq 0}$ designed to model interaction and to be explained in d) below, we define the i-th neuron $\mathcal{N}^{(i)}$ in the circuit, $1 \leq i \leq N$, as a stochastic process

$$\mathcal{N}^{(i)} := \left(V^{(i)}, n^{(i)}, m^{(i)}, h^{(i)}, X^{(i)}\right)$$

governed by a stochastic Hodgkin-Huxley equation of form

$$\begin{cases} dV_t^{(i)} &= A_t^{(i)}dt + dX_t^{(i)} - F(V_t^{(i)}, n_t^{(i)}, m_t^{(i)}, h_t^{(i)})dt \\ dn_t^{(i)} &= [\alpha_n(V_t^{(i)})(1 - n_t^{(i)}) - \beta_n(V_t^{(i)})n_t^{(i)}]dt \\ dm_t^{(i)} &= [\alpha_m(V_t^{(i)})(1 - m_t^{(i)}) - \beta_m(V_t^{(i)})m_t^{(i)}]dt \\ dh_t^{(i)} &= [\alpha_h(V_t^{(i)})(1 - h_t^{(i)}) - \beta_h(V_t^{(i)})h_t^{(i)}]dt. \end{cases} \tag{6.11}$$

On the long time behaviour of stochastic Hodgkin-Huxley neurons

c) Write $(\tau_n^{(j)})_{n\in\mathbb{N}}$ for the sequence of spike times of neuron $\mathcal{N}^{(j)}$, and associate a counting process $N^{(j)} = (N_t^{(j)})_{t\geq 0}$ to $(\tau_n^{(j)})_n$. From $N^{(j)}$ we define an output process $U^{(j)}$ for neuron $\mathcal{N}^{(j)}$

$$dU_t^{(j)} = -c_1 U_{t-}^{(j)} dt + dN_t^{(j)}, t \geq 0 \tag{6.12}$$

and stress that we use for all $1 \leq j \leq N$ the same decay parameter $c_1 \approx c^*$ selected as in modelization step 6.3. This implies that for all neurons $\mathcal{N}^{(j)}$, the same benchmarks (6.5) define an interval (u_1^*, u_2^*) over which values of $U^{(j)}$ are expected to fluctuate in case of regular spiking once time is large enough.

d) At this stage, the structure of the processes $A^{(i)}$ in (6.11) can be specified as follows:

$$A_t^{(i)} := \Phi_{\text{exc}}\left(U_{t-}^{(i-1)}\right) \quad , \quad i \in I_{\text{exc}},$$
$$A_t^{(i)} := \Phi_{\text{inh}}\left(U_{t-}^{(i-1)}\right) \quad , \quad i \in I_{\text{inh}}.$$

Here we use (6.12), (6.6)–(6.7), (6.10), and count modulo N around the circuit (6.8). In particular, at time t, neuron $\mathcal{N}^{(1)}$ depends via

$$A_t^{(1)} = \Phi_{\text{inh}}\left(U_{t-}^{(N)}\right)$$

on the output of neuron $\mathcal{N}^{(N)}$ immediately before time t.

e) To initialize the circuit (6.8), we sample starting values

 i) $X_0^{(i)}$ –for the Ornstein-Uhlenbeck processes in a)– from the invariant law $\mathcal{N}(0, \frac{\sigma^2}{2\tau})$, independently for all neurons;
 ii) $(V_0^{(i)}, n_0^{(i)}, m_0^{(i)}, h_0^{(i)})$ –for the biological variables in b)– from the uniform law on $(-12, 120)\times(0,1)$, independently for all neurons;
 iii) $U_0^{(i)}$ –for the output processes in c)– either: as random variables

$$U_0^{(j)} \text{ independent}, 1 \leq j \leq N, \text{ and distributed uniformly on } (1, u_1^*), \tag{6.13}$$

 or: deterministically
$$U_0^{(j)} := 0 \quad \text{for all} \quad j = 1, \ldots, N. \tag{6.14}$$

 iv) In a last step, given the values selected in iii) and defining by convention $U_{0-}^{(i-1)} := U_0^{(i-1)}$, we determine starting values $A_0^{(i)}$ for the input processes in (6.11), depending on the output $U_{0-}^{(i-1)}$ of the predecessor of neuron $\mathcal{N}^{(i)}$ and on its position in the circuit, according to d) above.

This finishes the initialization of the circuit (6.8).

We now explain why and in which sense circuits constructed as explained in modelization steps 6.1, 6.3, 6.4, 6.5 will exhibit auto-generated rhythmic oscillation of spiking activity around the circuit. There is strong evidence from simulations, see figures 7 and 8 as two examples. We have no rigorous proofs so far.

Remark 6.6. We explain the behaviour of the circuit in the following points i)–v):

 i) For a neuron $\mathcal{N}^{(i)}$ whose predecessor belongs to the same block, i.e. for $\mathcal{N}^{(i)}$ with index $i \in I_{\text{exc}}$:

α) Regular spiking of the predecessor $\mathcal{N}^{(i-1)}$ over some amount of time drives values of its output process $U^{(i-1)}$ into neighbourhoods of the interval (u_1^*, u_2^*), hence values of $A^{(i)} = \Phi_{\text{exc}}(U^{(i-1)})$ towards ϑ_2. Quite rapidly, this will force $\mathcal{N}^{(i)}$ into a regime of regular spiking.

β) Quiet behaviour of the predecessor $\mathcal{N}^{(i-1)}$ over some amount of time forces its output $U^{(i-1)}$ exponentially fast towards 0, hence values of $A^{(i)} = \Phi_{\text{exc}}(U^{(i-1)})$ towards ϑ_1. As a consequence, neuron $\mathcal{N}^{(i)}$ will soon be silenced and enter the quiet regime.

ii) For a neuron $\mathcal{N}^{(i)}$ which occupies the first place in its block, i.e. for $\mathcal{N}^{(i)}$ with index $i \in I_{\text{inh}}$:

α) Regular spiking of the predecessor over some amount of time drives its output $U^{(i-1)}$ into neighbourhoods of the interval (u_1^*, u_2^*), hence values of $A^{(i)} = \Phi_{\text{inh}}(U^{(i-1)})$ down to ϑ_1. As a consequence, neuron $\mathcal{N}^{(i)}$ will be silenced and enter the quiet regime.

β) Quiet behaviour of the predecessor over some amount of time forces its output $U^{(i-1)}$ towards 0, hence values of $A^{(i)} = \Phi_{\text{inh}}(U^{(i-1)})$ towards ϑ_2. As a consequence, neuron $\mathcal{N}^{(i)}$ will be forced into a regime of regular spiking.

iii) When the blocks have suitable length L, the following happens inside every block:

α) excitation of successor neurons as in i α) tends to propagate through the block as a whole (i.e. with high probability, the neuron in the last position of the block will get excited before randomness might generate other patterns), and finally all neurons in this block will be regularly spiking;

β) silencing of successor neurons as in i β) tends to propagate through the block as a whole (with analogous caveat), and finally all neurons in the block will be silenced.

Thus a pattern distinguishing active blocks from quiet blocks will appear in the circuit.

iv) Consider neurons $\mathcal{N}^{(i)}$ which occupy the first position $i \in I_{\text{inh}}$ in their block. Then together with $\mathcal{N}^{(i)}$, the block as a whole –as described in iii)– will 'flip' whenever the following happens :

α) From active to quiet, given that the block so far was regularly spiking: at the time where activity propagating through the preceding block reaches position $i-1 \in I_{\text{exc}}$ and thus excites neuron $\mathcal{N}^{(i-1)}$, input $A^{(i)} = \Phi_{\text{inh}}(U^{(i-1)})$ will break down (as a consequence of growing output $U^{(i-1)}$ since $i \in I_{\text{inh}}$), thus neuron $\mathcal{N}^{(i)}$ will be forced into silence.

β) From quiet to active, given that the block so far was quiet: at the time where silence propagating through the preceding block attains position $i-1$ and silences neuron $\mathcal{N}^{(i-1)}$, input $A^{(i)} = \Phi_{\text{inh}}(U^{(i-1)})$ will increase for position i (as a consequence of decreasing output $U^{(i-1)}$ since $i \in I_{\text{inh}}$), thus neuron $\mathcal{N}^{(i)}$ will be forced into regular spiking regime. In both cases, by iii), silence of $\mathcal{N}^{(i)}$ or activity of $\mathcal{N}^{(i)}$ will propagate over the corresponding block.

v) The number M of blocks being odd by assumption in modelization step 6.5, stable coexistence in equal number of blocks which are permanently quiet alternating with blocks which are permanently active is impossible; in permanence, blocks will be obliged to 'flip' when either some active block is approached from the left by

propagating activity, or some silent block is approached from the left by silence. By 'flipping' of suitable blocks at suitable times, the pattern of alternating active and quiet regions around the circuit performs some kind of counter-clockwise rotation which looks very much like a periodic phenomenon.

Figures 7 and 8 below illustrate how oscillating activity patterns according to blocks in circuits described in modelization steps 6.1, 6.3, 6.4, 6.5 appear and stabilize in a slow rhythmic rotation around the circuit. Both figures use the same delay parameter c_1 chosen according to (6.5), and the same parameter values for τ and σ chosen as in modelization step 6.1. The choice of starting values for the collection of output processes is somewhat different: figure 7 has $U_0^{(j)} = 0$ for all j as in (6.14), and figure 8 selects for all j an initial position uniformly on $(1, u_1^*)$ as in (6.13). In both cases, after some initial phase of randomness which prevails in all blocks, spiking activity in one block turns out to be strong enough to silence its successor block, thus initializing a rotative motion of silent and active regions along the circuit.

Remark 6.7. With reference to Ditlevsen and Löcherbach [4], we discuss a deterministic reference model which explains why we expect the self-organized rhythmic behaviour of the system constructed in modelization step 6.5 –illustrated by figures 7 and 8, and explained in remark 6.6– to be persistent in the long run, certainly from time to time perturbed in a random way but always restoring itself rapidly in the sequel. The reference model is a simplified special case of the deterministic limit model in [4].

Think of a deterministic system of dimension $N = ML$ where real-valued variables $t \to x_i(t)$ represent in some way a spiking activity of neuron i as a function of time, with neurons arranged as a circuit of M blocks of L neurons, and where counting modulo N the interaction is of type

$$\frac{dx_i}{dt}(t) = \begin{cases} -cx_i(t) - f(x_{i-1}(t)) & \text{if } i \in \mathbb{I}_{\text{inh}} \\ -cx_i(t) + f(x_{i-1}(t)) & \text{if } i \in \mathbb{I}_{\text{exc}} \end{cases}$$

with f some smoothed version of the truncated identity $x \to (x \vee -1) \wedge 1$, and $c \in (0, 1)$ some constant. As in (6.10), indices $\mathbb{I}_{\text{inh}}$ correspond to neurons which occupy the first position in their block.

Under the condition that i) M is odd and ii) c is small enough, this system evolves on a finite number of periodic orbits, and at least one periodic orbit is stable. This follows from Theorem 3 in Section 4 of [4]. Random initial conditions in this deterministic model $((x_1(0), \ldots, x_N(0))$ drawn from a uniform law on $(-1, 1)^N)$ produce activity patterns very similar to what we see in figures 7 and 8.

Remark 6.8. We emphasize that modelization step 6.1 requires regular spiking under ϑ_2 and quiet behaviour under ϑ_1, both with probability close to 1, under the same pair (τ, σ) governing the Ornstein-Uhlenbeck noise in all neurons. Choice of (τ, σ) is of key importance for the feature of self-organized oscillation in systems constructed in modelization steps 6.1, 6.3, 6.4, 6.5 of interacting stochastic Hodgkin-Huxley models. The feature of interest –self-organized slow rhythmic oscillation of activity patterns around the circuit– will be destroyed when the volatility σ becomes too large or the back-driving force τ too small: then for all neurons in the circuit, the spiking activity will be more or less irregular or chaotic. In this sense, Definitions 4.1 and 5.1 are of key importance for our construction.

7 Appendix : details for some proofs in Section 3

Fix ϑ, τ and σ and suppress corresponding superscripts ($Q_x = Q_x^{(\vartheta, \tau, \sigma)}$, $E_\mu = E_\mu^{(\vartheta, \tau, \sigma)}$, etc.).

spike trains in circuit of 12 neurons, inhibited (red) or excited (green) by predecessor (OU sigma = 1.5 , tau = 1.4)
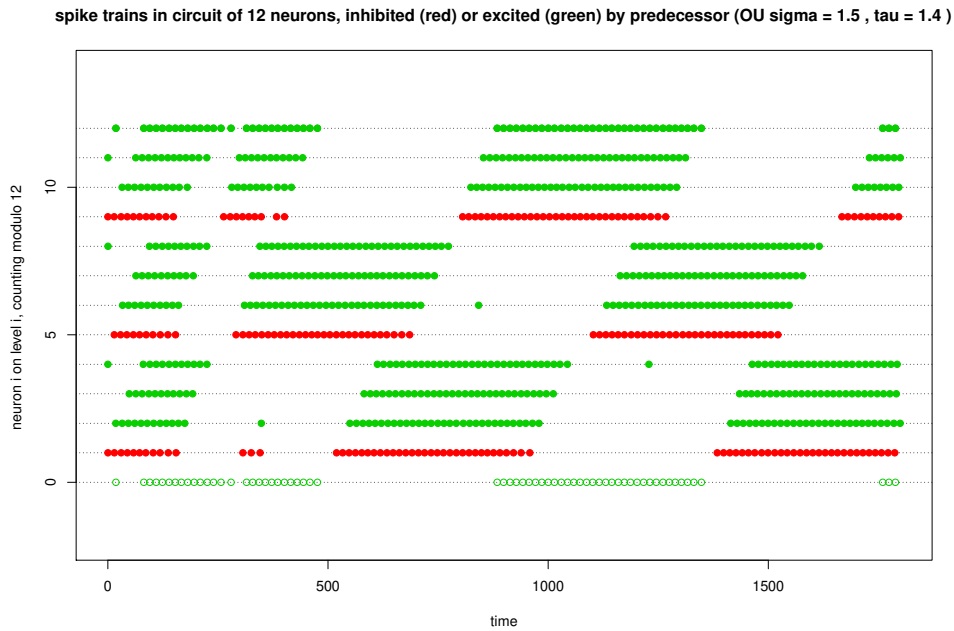

Figure 7: Simulation of a circuit described in modelization steps 6.1, 6.3, 6.4 and 6.5 up to time 1800, using Euler schemes of step size 0.001, with $N = 12$ neurons in $M = 3$ blocks of $L = 4$ cells. We show the spike times of all neurons, with neuron $\mathcal{N}^{(i)}$ represented at horizontal level i, and $\mathcal{N}^{(12)} = \mathcal{N}^{(0)}$ represented twice to visualize the cyclic structure. We use red dots for positions $i \in \mathbb{I}_{\mathrm{inh}}$, green dots for $i \in \mathbb{I}_{\mathrm{exc}}$. 'Noise' has parameter values $\sigma = 1.5$ and $\tau = 1.4$, as in Example 6.2. The decay parameter $c_1 = 0.02$ for output processes satisfies (6.5), we have $\Delta^* \approx 14.3$ in (6.3) and $u_1^* \approx 3.01$ in (6.4). Initial conditions for output processes are (6.14): $U_0^{(j)} = 0$ for all j. Thus the input processes $A^{(i)}$ start at $\vartheta_2 = 10$ for $i \in \mathbb{I}_{\mathrm{inh}}$, and at $\vartheta_1 = 4$ for $i \in \mathbb{I}_{\mathrm{exc}}$; this gives a slight 'advantage' to positions $i \in \mathbb{I}_{\mathrm{inh}}$ which tend to spike earlier, exciting successor neurons in the same block. In the initial phase of this simulation, the block $\{9, 10, 11, 12\}$ is the first which succeeds in silencing its successor block.

Under the lower bound condition given by Theorem 3.1 d), with T, α, ν and C as there, Nummelin splitting in the grid chain $(\mathbb{X}_{kT})_{k \in \mathbb{N}_0}$ works as follows. Prepare i.i.d. random variables $(V_k)_{k \in \mathbb{N}_0}$, uniformly distributed on $(0, 1)$, and independent of the process $(\mathbb{X}_{kT})_{k \in \mathbb{N}_0}$. Whenever the grid chain enters the 'small set' C at a time k in a state $x \in C$, we split the transition away from x according to the value of V_k: on $\{V_k < \alpha\}$, we select the successor state y for x according to $\nu(dy)$; on $\{V_k \geq \alpha\}$, we select y according to the probability measure $\frac{P_T(x,dy) - \alpha\nu(dy)}{1-\alpha}$. Apply colors as follows: on $\{V_k < \alpha\}$ we color (k, x) 'red' and $(k+1, y)$ 'green'; on $\{V_k \geq \alpha\}$ we color both (k, x) and $(k+1, y)$ 'blue'. All other transitions remain uncolored. This amounts to an extension of the underlying probability space such that for the 'colored' grid chain $(\mathbb{X}_{kT})_{k \in \mathbb{N}_0}$, the set of 'green' time points defines a sequence of renewal times where the grid chain starts afresh from law ν. This is Nummelin [19]. If we define

$$R_0 \equiv 0 \quad , \quad R_{n+1} := \inf\{k > R_n : \mathbb{X}_{kT} \in C \ \text{ and } \ V_k < \alpha\}, n \in \mathbb{N}_0,$$
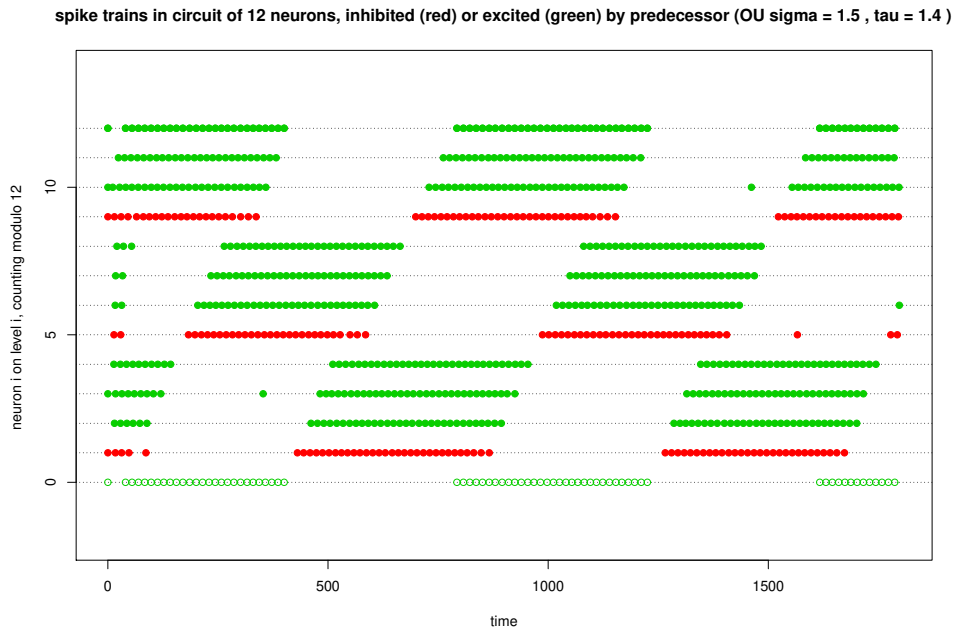
Figure 8: Simulation of a circuit with the same structure and the same parameters as in figure 7, except that now we use random initial conditions (6.13) for the output processes: for all j, $U_0^{(j)}$ is distributed uniformly on $(1, u_1^*)$. Quite rapidly, the circuit organizes itself in patterns which block-wise perform a slow rotation around the circuit.

then $(R_n)_n$ is a sequence of stopping times with respect to the discrete filtration

$$\check{\mathbb{F}} = (\check{\mathcal{F}}_k)_{k \in \mathbb{N}_0} \quad , \quad \check{\mathcal{F}}_k := \sigma \left(\mathbb{X}_{jT}, V_j : 0 \le j \le k \right).$$

Harris recurrence implies $R_n \uparrow \infty$ almost surely as $n \to \infty$. In discrete time, successive path segments from 'green' to subsequent 'red' times (i.e. from $R_n + 1$ to R_{n+1}, $n \in \mathbb{N}$) decompose the trajectory of $(\mathbb{X}_{kT}^{(\vartheta)})_{k \in \mathbb{N}_0}$ into i.i.d. excursions which we call life cycles, up to some initial segment. Positive Harris recurrence by Theorem 3.1 grants that the expected length $E_\bullet(R_2 - R_1)$ of a life cycle is finite (and independent of the starting point of $\mathbb{X}$).

In continuous time we consider the filtration

$$\mathbb{F} := (\mathcal{F}_t)_{t \ge 0} \quad , \quad \mathcal{F}_t := \bigcap_{r > t} \mathcal{F}_r^\circ \quad , \quad \mathcal{F}_t^\circ := \{ \mathbb{X}_s, s \le t, V_j, jT \le t \} \tag{7.1}$$

generated by the pair

$$\left(\mathbb{X}^{(\vartheta)}, \sum_j V_j \mathbb{1}_{[\![jT, (j+1)T [\![}} \right),$$

with T as above. Then $(R_n T)_{n \in \mathbb{N}}$ is a sequence of $\mathbb{F}$-stopping times increasing to ∞. If we think of the continuous-time process in terms of bridges pasted into the grid chain, Nummelin splitting in the grid chain with coloring as above shows that path segments

$$\mathbb{X} \mathbb{1}_{[\![(R_n + 1)T, R_{n+1}T]\!]} \quad , \quad n \in \mathbb{N} \tag{7.2}$$

from 'green' to subsequent 'red' times are i.i.d. in the continuous-time setting ([10]); note that here we do leave out a short piece of trajectory from 'red' to 'green', of length

T, for all n. For all $n \in \mathbb{N}$, the $\mathbb{F}$-stopping times $(R_n+1)T$ are renewal times where the process starts anew from initial law ν; the future following time $(R_n+1)T$ is independent from the past $\mathcal{F}_{R_nT}$ up to time R_nT.

When we prefer to consider path segments 'from green to green'

$$\mathbb{X}\mathbb{1}_{[\![(R_j+1)T,(R_{j+1}+1)T[\![} \quad , \quad j \in \mathbb{N}, \tag{7.3}$$

then these also are identical in law, but independence holds only two-by-two (cf. Löcherbach and Loukianova [17]): those with j even are i.i.d., and –separately– those with j odd. The same reasoning shows that for every $K \in \mathbb{N}$ which we keep fixed, path segments 'from green to green over $K-1$ renewal intervals'

$$\mathbb{X}\mathbb{1}_{[\![(R_{jK+r}+1)T,(R_{(j+1)K+r-1}+1)T[\![} \quad , \quad 0 < r \leq K, j \in \mathbb{N}_0 \tag{7.4}$$

are identical in law, but independence holds K-by-K only: fixing r, path segments

$$\mathbb{X}\mathbb{1}_{[\![(R_{jK+r}+1)T,(R_{(j+1)K+r-1}+1)T[\![} \quad , \quad j \in \mathbb{N}_0 \tag{7.5}$$

are independent when $0 < r \leq K$ is fixed. We shall speak of (7.3) or of (7.4) as life cycles.

Lemma 7.1. *Fix a natural number $L > 1$. For every point $v = (v_1, v_2, \ldots, v_L) \in [0,\infty)^L$, with notation $[0,v] := \overset{L}{\underset{i=1}{\mathsf{X}}}[0,v_i]$, and every function $h : [0,\infty)^L \to \mathbb{R}$ which is measurable and bounded, writing $\mathbb{1}_{[0,v]}h$ for the product $\mathbb{1}_{[0,v]} \cdot h$, we have almost sure convergence of*

$$\widehat{G}_m(v,h) := \frac{1}{m}\sum_{n=1}^{m}\left(\mathbb{1}_{[0,v]}h\right)(\tau_{n+1}-\tau_n,\ldots,\tau_{n+L}-\tau_{n+L-1}) \tag{7.6}$$

to a deterministic limit as $m \to \infty$.

Proof. We modify the proof of Theorem 2.9 in [13], section 5.

1) We count spikes in the life cycles (7.3):

$$\widetilde{Z}_j := \sum_{n=1}^{\infty}\mathbb{1}_{\{(R_j+1)T \leq \tau_n < (R_{j+1}+1)T\}} \quad , \quad j \in \mathbb{N}. \tag{7.7}$$

Since interspike times are $> \delta_0$ by construction, $\widetilde{Z}_j$ is upper bounded by $\frac{1}{\delta_0}(R_{j+1}-R_j)T$ which has finite expectation. Thus the $(\widetilde{Z}_j)_j$, identical in law, belong to $L^1(Q_\mu)$, and are independent two-by-two using (7.3). As a consequence,

$$\lim_{m\to\infty}\frac{1}{2m}\sum_{j=1}^{2m}\widetilde{Z}_j = \frac{1}{2}\lim\frac{1}{m}\sum_{j=1}^{m}\widetilde{Z}_{2j} + \frac{1}{2}\lim\frac{1}{m}\sum_{j=0}^{m-1}\widetilde{Z}_{2j+1} = E_\bullet\left(\widetilde{Z}_1\right)$$

exists almost surely, and thus also $\lim\frac{1}{m}\sum_{j=1}^{m}\widetilde{Z}_j$. The limit does not depend on the starting point. Now asymptotically as $m \to \infty$

$$\begin{aligned}\frac{1}{m}\sum_{j=1}^{m}\widetilde{Z}_m &= \frac{1}{m}\cdot\text{number of spikes in }[\![(R_1+1)T,(R_{m+1}+1)T[\![\\ &= \frac{1}{m}\cdot\text{number of spikes in }]\!](R_1+1)T,(R_{m+1}+1)T[\![+ o_{Q_x}(1) \\ &= \frac{1}{m}\cdot\text{number of spikes in }]\!]0,(R_{m+1}+1)T[\![+ o_{Q_x}(1) \\ &= \frac{1}{m}N_{(R_{m+1}+1)T} + o_{Q_x}(1)\end{aligned}$$

whence with the help from Proposition 3.4

$$E_\mu\left(\widetilde{Z}_1\right) = \lim_{m\to\infty} \frac{1}{m}\sum_{j=1}^m \widetilde{Z}_j = T E_\mu(N_1) E_\mu(R_2 - R_1). \tag{7.8}$$

2) Fix $v = (v_1, v_2, \ldots, v_L) \in [0,\infty)^L$ and $h : [0,\infty)^L \to \mathbb{R}$ measurable and bounded, and consider

$$Z_j(v,h) := \sum_{n=1}^\infty \mathbb{1}_{\{(R_j+1)T \le \tau_n < (R_{j+1}+1)T\}} \left(\mathbb{1}_{[0,v]}h\right)(\tau_{n+1} - \tau_n, \ldots, \tau_{n+L} - \tau_{n+L-1}) \tag{7.9}$$

for $j \in \mathbb{N}$. Then the $(Z_j(v,h))_j$ are identical in law, and belong to $L^1(Q_\mu)$ by comparison with (7.7). We shall show in two steps –2i) and 2ii) below– that the variables $(Z_j(v,h))_j$ in (7.9) are independent K-by-K provided we choose $K \in \mathbb{N}$ large enough, i.e. for

$$K \ge 2 + \frac{1}{T}\sum_{i=1}^L v_i. \tag{7.10}$$

i) In (7.9) we have to consider events

$$B(j,n) := \{(R_j+1)T \le \tau_n < (R_{j+1}+1)T\} \bigcap \bigcap_{i=1}^L \{\tau_{n+i} - \tau_{n+i-1} \in [0,v_i]\}$$

on which

$$\tau_{n+L} = \tau_n + \sum_{i=1}^L (\tau_{n+i} - \tau_{n+i-1}) < (R_{j+1}+1)T + \sum_{i=1}^L v_i;$$

thus with the choice (7.10), the following holds on $B(j,n)$:

$$\tau_{n+L} < (R_{j+1}+1)T + (K-2)T = (R_{j+1}+K-1)T < R_{j+K}T.$$

ii) Now

$$\{(R_j+1)T \le \tau_n < (R_{j+1}+1)T\} \in \mathcal{F}_{\tau_n}$$

and $(\tau_j)_j$ is an increasing sequence of $\mathbb{F}$-stopping times: thus the event $B(j,n)$ belongs to the σ-field $\mathcal{F}_{R_{j+K}T}$ of events up to time $R_{j+K}T$. Since the last σ-field does not depend on n, the definition (7.9) grants that for every $j \in \mathbb{N}$,

$$\text{the variable } Z_j(v,h) \text{ is measurable with respect to } \mathcal{F}_{R_{j+K}T} \tag{7.11}$$

whereas the construction of the renewal times $(R_j+1)T$ for the continuous-time process $\mathbb{X}$ implies

$$\text{the variable } Z_j(v,h) \text{ is independent of } \mathcal{F}_{R_jT} \tag{7.12}$$

for all j. As a consequence, the family $(Z_j(v,h))_j$ is independent K-by-K as asserted since we have for every $0 < r \le K$ independence in restriction to the subfamily $\{Z_{\ell K+r}(v,h), \ell \in \mathbb{N}_0\}$.

3) The $(Z_j(v,h))_j$ being identical in law and independent K-by-K, a deterministic limit

$$\lim_{m\to\infty} \frac{1}{m}\sum_{j=1}^m Z_j(v,h) = \lim_{m\to\infty} \frac{1}{mK}\sum_{j=1}^{mK} Z_j(v,h)$$

$$= \frac{1}{K}\sum_{r=1}^K \left(\lim_{m\to\infty} \frac{1}{m}\sum_{\ell=0}^{m-1} Z_{\ell K+r}(v,h)\right) = E_\mu(Z_1(v,h))$$

exists almost surely, by the classical strong law of large numbers. This is the essential step in the proof of the lemma.

4) Asymptotically as $m \to \infty$ we can write

$$\frac{1}{m}\sum_{j=1}^{m} Z_j(v,h)$$

in the following form:

$$\frac{1}{m}\sum_{j=1}^{m}\sum_{n=1}^{\infty}\mathbb{1}_{\{(R_j+1)T \le \tau_n < (R_{j+1}+1)T\}}\left(\mathbb{1}_{[0,v]}h\right)(\tau_{n+1}-\tau_n,\ldots,\tau_{n+L}-\tau_{n+L-1})$$

$$=\frac{1}{m}\sum_{n=1}^{\infty}\mathbb{1}_{\{(R_1+1)T \le \tau_n < (R_{m+1}+1)T\}}\left(\mathbb{1}_{[0,v]}h\right)(\tau_{n+1}-\tau_n,\ldots,\tau_{n+L}-\tau_{n+L-1})$$

$$=\frac{1}{m}\sum_{n=N_{(R_1+1)T}+1}^{N_{(R_{m+1}+1)T}}\left(\mathbb{1}_{[0,v]}h\right)(\tau_{n+1}-\tau_n,\ldots,\tau_{n+L}-\tau_{n+L-1})+o_{Q_x}(1)$$

$$=\frac{1}{m}\sum_{n=1}^{N_{(R_{m+1}+1)T}}\left(\mathbb{1}_{[0,v]}h\right)(\tau_{n+1}-\tau_n,\ldots,\tau_{n+L}-\tau_{n+L-1})+o_{Q_x}(1)$$

$$=\frac{N_{(R_{m+1}+1)T}}{m}\widehat{G}_{N_{(R_{m+1}+1)T}}(v,h)+o_{Q_x}(1)$$

$$=TE_\mu(N_1)E_\mu(R_2-R_1)\widehat{G}_{N_{(R_{m+1}+1)T}}(v,h)+o_{Q_x}(1)$$

with the help from Proposition 3.4 and since $h:[0,\infty)^L \to \mathbb{R}$ is bounded. From the last line and step 3) it follows that

$$\lim_{m\to\infty}\widehat{G}_{N_{(R_{m+1}+1)T}}(v,h) \tag{7.13}$$

exists almost surely and equals

$$E_\mu(Z_1(v,h))/(TE_\mu(N_1)E_\mu(R_2-R_1)) \quad = \quad E_\mu(Z_1(v,h))/E_\mu\left(\widetilde{Z}_1\right) \tag{7.14}$$

with reference to step 1). Decomposing h into positive and negative part shows that it is sufficient to consider $h \ge 0$: but then, existence of the limit in (7.13) is equivalent to existence of the limit

$$\lim_{m\to\infty}\widehat{G}_m(v,h) \tag{7.15}$$

almost surely, and the proof of the lemma is finished.

$\square$

Remark 7.2. The almost sure limit in Lemma 7.1 and in (7.13)–(7.15) of its proof

$$E_\mu(Z_1(v,h))/E_\mu\left(\widetilde{Z}_1\right)=\lim_{m\to\infty}\widehat{G}_m(v,h)$$

admits an interpretation: it equals the relative number of spikes in the long run for which subsequent L interspike times realize a particular pattern, expressed by the function $\mathbb{1}_{[0,v]}h$,

$$\lim_{t\to\infty}\frac{1}{N_t}\sum_{n=1}^{N_t}\left(\mathbb{1}_{[0,v]}h\right)(\tau_{n+1}-\tau_n,\ldots,\tau_{n+L}-\tau_{n+L-1}) \tag{7.16}$$

(considering $h \ge 0$ first, (7.16) is a consequence of (7.15) exactly as (7.15) was a consequence of (7.13) in step 4) of the proof of Lemma 7.1), and it equals –in terms of life cycles, cf. (7.9) and (7.3)– the ratio

$$\frac{E_\mu\left(\sum_{n=1}^{\infty}\mathbb{1}_{\{(R_1+1)T\le\tau_n<(R_2+1)T\}}\left(\mathbb{1}_{[0,v]}h\right)(\tau_{n+1}-\tau_n,\ldots,\tau_{n+L}-\tau_{n+L-1})\right)}{E_\mu\left(\sum_{n=1}^{\infty}\mathbb{1}_{\{(R_1+1)T\le\tau_n<(R_2+1)T\}}\right)} \tag{7.17}$$

between the expected number of spikes in a life cycle for which subsequent L interspike times realize this particular pattern, divided by the expected number of spikes in the life cycle.

Proof for Theorem 3.5. The special case $h \equiv 1$ in Lemma 7.1 establishes pointwise convergence on $[0, \infty)^L$ of empirical distribution functions $\widehat{G}_m(\cdot) := \widehat{G}_m(\cdot, h \equiv 1)$ associated to the first m observed L-tuples of successive interspike times

$$(\tau_{n+1} - \tau_n, \ldots, \tau_{n+L} - \tau_{n+L-1}) \quad , \quad n \in \mathbb{N}$$

in (3.14) to a limit $G_\mu(\cdot)$. The proof of Lemma 7.1, or Remark 7.2, identifies the limit as

$$G_\mu(v) := E_\mu \left(Z_1(v, h \equiv 1) \right) / E_\mu \left(\widetilde{Z}_1 \right) \quad , \quad v \in [0, \infty)^L$$

where $Z_1(v, h \equiv 1)$ and $\widetilde{Z}_1$ are given by (7.9) and (7.7). By (7.17), with $h \equiv 1$ and $v = (v_1, \ldots, v_L)$,

$$G_\mu(v) = \frac{E_\mu \left(\sum_{n=1}^\infty \mathbb{1}_{\{(R_1+1)T \leq \tau_n < (R_2+1)T\}} \mathbb{1}_{[0,v_1]}(\tau_{n+1} - \tau_n) \cdots \mathbb{1}_{[0,v_L]}(\tau_{n+L} - \tau_{n+L-1}) \right)}{E_\mu \left(\sum_{n=1}^\infty \mathbb{1}_{\{(R_1+1)T \leq \tau_n < (R_2+1)T\}} \right)}.$$

Interspike times are $> \delta_0$ by construction, are finite, and a life cycle contains a finite number of spikes: so the last representation shows that $G_\mu(\cdot)$ is the distribution function of a probability measure on $[0, \infty)^L$, clearly concentrated on $(0, \infty)^L$. Pointwise convergence $\widehat{G}_m \to G_\mu$ on $[0, \infty)^L$ being established, uniformity on $[0, \infty)^L$ follows as in classical proofs of the Glivenko-Cantelli Theorem on $\mathbb{R}^L$. Theorem 3.5 is proved. $\qquad \square$

Remark 7.3. a) The product $\mathbb{1}_{[0,v]} h$ in Lemma 7.1 allows to study the relative frequencies in the long run of particular patterns in groups of L successive interspike times. As an example, consider points v in $[0, \infty)^L$ such that $v_1 = v_2 = \ldots = v_L =: \bar{v}$ is sufficiently large, and let h denote the indicator of events in L-point data sets such that 'the distance between upper and lower 10% quantiles does not exceed 5% of the median'. Then $G_\mu(v, h)$ gives the proportion of spike times τ_n in the long run which are to be followed by interspike times $(\tau_{n+1} - \tau_n, \ldots, \tau_{n+L} - \tau_{n+L-1})$ with the following two properties: i) the interspike times do not exceed $\bar{v}$; ii) the interspike times cluster in the above sense in small neighbourhoods of their median. Under this (or similar) definition of h, spikes will look close-to-equally spaced over large periods of time whenever $G_\mu(v, h)$ is close to one. $\widehat{G}_m(v, h)$ gives the relative frequency of the pattern encoded in $\left(\mathbb{1}_{[0,v]} h \right)$ in observed spike trains of length m. While we have probably no chance to calculate $G_\mu(\cdot, h)$ in the sense of an explicit and closed-form expression, we may replace it with $\widehat{G}_m(\cdot, h)$ when m is large. Thus Lemma 7.1 provides us –asymptotically as $m \to \infty$– with tools in view of statistical inference.

b) We emphasize that the renewal techniques in the proof of Lemma 7.1 build on presence of an indicator $\mathbb{1}_{[0,v]}$ in the product $\mathbb{1}_{[0,v]} h$: this indicator can not be omitted.

Proof for Proposition 3.6: Fix $\varepsilon > 0$. Choose L large enough for $\sum_{\ell > L} e^{-c_1 \delta_0 \ell} < \varepsilon$. For every $n \in \mathbb{N}$, the pair $\left(U_{\tau_{n+L}}, U_{(\tau_{n+L+1})^-} \right)$ to be considered in (3.17)

$$U_{\tau_{n+L}} = \sum_{j=1}^{n+L} e^{-c_1(\tau_{n+L} - \tau_j)} = \sum_{\ell=1-n}^{L} e^{-c_1(\tau_{n+L} - \tau_{n+\ell})}$$

$$U_{(\tau_{n+L+1})^-} = U_{\tau_{n+L}} e^{-c_1(\tau_{n+L+1} - \tau_{n+L})} = \sum_{\ell=1-n}^{L} e^{-c_1(\tau_{n+L+1} - \tau_{n+\ell})}$$

will be approximated with the help of truncated sums by

$$V_n \quad := \quad \sum_{j=n}^{n+L} e^{-c_1(\tau_{n+L}-\tau_j)} = \sum_{\ell=0}^{L} e^{-c_1(\tau_{n+L}-\tau_{n+\ell})}$$

$$V_{n+1}^- \quad := \quad V_n e^{-c_1(\tau_{n+L+1}-\tau_{n+L})} = \sum_{\ell=0}^{L} e^{-c_1(\tau_{n+L+1}-\tau_{n+\ell})}.$$

This pair $\left(V_n, V_{n+1}^-\right)$ appears as approximation (3.18) in Proposition 3.6.

1) Since interspike times are $> \delta_0$ by construction in (3.10), we have geometric bounds

$$0 < U_{\tau_{n+L}} - V_n < \sum_{\ell>L} e^{-c_1\ell\delta_0} < \varepsilon \quad , \quad 0 < U_{(\tau_{n+L+1})^-} - V_{n+1}^- < \sum_{\ell>L} e^{-c_1(\ell+1)\delta_0} < \varepsilon$$

uniformly in n. This is the first assertion in Proposition 3.6.

2) Consider points $x = (x_1,\ldots,x_{L+1})$ in $[\delta_0,\infty)^{L+1}$, with δ_0 from (3.10). With c_1 from (3.15) or (3.16), we define continuous functions

$$\begin{aligned} f_1: \quad x \quad &\longrightarrow \quad e^{-c_1(x_L+\ldots+x_1)} + e^{-c_1(x_L+\ldots+x_2)} + \ldots + e^{-c_1 x_L} + 1 \\ f_2: \quad x \quad &\longrightarrow \quad e^{-c_1(x_{L+1}+\ldots+x_1)} + e^{-c_1(x_{L+1}+\ldots+x_2)} + \ldots + e^{-c_1(x_{L+1}+x_L)} + e^{-c_1 x_{L+1}} \end{aligned}$$

which on $[\delta_0,\infty)^{L+1}$ are bounded by $\sum_{\ell\geq0} e^{-c_1\ell\delta_0}$ (the last bound does not depend on L). Interspike times being $> \delta_0$ by construction, we have

$$\begin{aligned} V_n &= f_1\left(\tau_{n+1}-\tau_n,\ldots,\tau_{n+L}-\tau_{n+L-1},\tau_{n+L+1}-\tau_{n+L}\right) \\ V_{n+1}^- &= f_2\left(\tau_{n+1}-\tau_n,\ldots,\tau_{n+L}-\tau_{n+L-1},\tau_{n+L+1}-\tau_{n+L}\right). \end{aligned}$$

We can extend f_1, f_2 to continuous and bounded functions $[0,\infty)^{L+1} \to \mathbb{R}$.

3) On $[0,\infty)^{L+1}$, we write indistinctly $\widehat{G}_m$ for the empirical distribution functions in Theorem 3.5 (with L to be replaced by $L+1$) and for the associated empirical measures

$$\frac{1}{m}\sum_{n=1}^{m} \epsilon_{(\tau_{n+1}-\tau_n,\ldots,\tau_{n+L}-\tau_{n+L-1},\tau_{n+L+1}-\tau_{n+L})} \quad , \quad m \to \infty.$$

By Theorem 3.5, empirical measures $\widehat{G}_m$ converge weakly in $[0,\infty)^{L+1}$ to G_μ as $m \to \infty$ (again we write G_μ both for the limiting probability measure on $[0,\infty)^{L+1}$ and for its distribution function). Introducing the continuous function

$$F := (f_1, f_2) : [0,\infty)^{L+1} \to [0,\infty)^2$$

the continuous mapping theorem shows that the empirical measures

$$\widehat{H}_m = \frac{1}{m}\sum_{n=1}^{m} \epsilon_{\left(V_n, V_{n+1}^-\right)} = \frac{1}{m}\sum_{n=1}^{m} \epsilon_{F(\tau_{n+1}-\tau_n,\ldots,\tau_{n+L}-\tau_{n+L-1},\tau_{n+L+1}-\tau_{n+L})}$$

on $[0,\infty)^2$, images of $\widehat{G}_m$ under F, converge weakly in $[0,\infty)^2$ to the probability measure H_μ

$$H_\mu(A) := G_\mu\left(F^{-1}(A)\right) \quad , \quad A \in \mathcal{B}([0,\infty)^2),$$

the image of G_μ under F. Weak convergence in $[0,\infty)^2$ can be reformulated in terms of distribution functions as asserted in Proposition 3.6.

$\square$

Remark 7.4. It is clear that –introducing some more indices– the last proof can be extended to deal with J-tuples (3.19)

$$\left(\left(U_{\tau_{n+j+L}}, U_{(\tau_{n+j+L+1})^-} \right)_{0 \le j \le J} \right) \quad , \quad n \in \mathbb{N}$$

as mentioned at the end of Section 3.3. The problem that we need huge values of L in order to obtain small values of ε remains the same. The limit law in such an extension of Proposition 3.6 has the interpretation of governing patterns in the output process which may be observed in the long run.

8 Appendix: a discussion of the benchmarks (5.7) in Section 5

As a complement to Section 5, we discuss –with notations of Section 5– the role of benchmarks (5.7) in connection with asymptotic properties of the sequence of events $R(T_1)$ as $T_1 \to \infty$.

Our discussion is based on two conjectures concerning the limit distribution $H^{(\vartheta,\tau,\sigma)}$ from Proposition 3.2 b) for the empirical distribution functions $\widehat{H}_n$ of the first n interspike times as $n \to \infty$.

Conjecture 8.1. *For all parameter values (ϑ,τ,σ), $H^{(\vartheta,\tau,\sigma)}$ is continuous and strictly monotone on its interval of support $(\alpha^{(\vartheta,\tau,\sigma)}, \beta^{(\vartheta,\tau,\sigma)})$ in $(0,\infty)$.*

In view of the second conjecture, write $\mathrm{q}^{(\vartheta,\tau,\sigma)}(\alpha) := \inf\{v > 0 : H^{(\vartheta,\tau,\sigma)}(v) \ge \alpha\}$ for quantiles of $H^{(\vartheta,\tau,\sigma)}$, $\Delta^{(\vartheta,\tau,\sigma)}$ for the median of $H^{(\vartheta,\tau,\sigma)}$, $\mathrm{d}^{(\vartheta,\tau,\sigma)}(\alpha)$ for the difference between upper and lower α-quantiles, and

$$\mathrm{r}^{(\vartheta,\tau,\sigma)}(\alpha) := \frac{\mathrm{d}^{(\vartheta,\tau,\sigma)}(\alpha)}{\Delta^{(\vartheta,\tau,\sigma)}}$$

for the ratio 'difference between upper and lower α-quantiles divided by the median' in $H^{(\vartheta,\tau,\sigma)}$.

Conjecture 8.2. *There are parameter triplets (ϑ,τ,σ) such that $H^{(\vartheta,\tau,\sigma)}$ satisfies*

$$\mathrm{r}^{(\vartheta,\tau,\sigma)}(0.05) < 0.3 \quad , \quad \mathrm{r}^{(\vartheta,\tau,\sigma)}(0.1) < 0.2 \quad , \quad \mathrm{r}^{(\vartheta,\tau,\sigma)}(0.25) < 0.1$$

together with

$$\left| E_\mu^{(\vartheta,\tau,\sigma)}(N_1) \Delta^{(\vartheta,\tau,\sigma)} - 1 \right| < 0.05$$

where we refer to the almost sure limit $\lim_{t\to\infty} \frac{N_t}{t}$ under (ϑ,τ,σ) in virtue of Proposition 3.4.

Even if we have no proof so far (the proofs for Proposition 3.2 b) –or for Theorem 3.5 in Section 7– yield existence of almost sure limits, and nothing more) we do not doubt that Conjecture 8.1 holds true for all parameter triplets (ϑ,τ,σ), and that Conjecture 8.2 holds true whenever the signal ϑ is large and –depending on the value of σ– the back-driving force τ is large enough or –depending on the value of τ– the volatility σ is small enough. As an example, both Conjectures 8.1 and 8.2 should hold true for the parameter triplets marked with an Asterisk * in the scheme of Example 5.2.

Proposition 8.3. *For parameter triplets (ϑ,τ,σ) satisfying both Conjectures 8.1 and 8.2, the event*

$$R(\infty) := \liminf_{T_1 \in \mathbb{N}, T_1 \to \infty} R(T_1)$$

in $\mathcal{G}_\infty = \mathcal{C}$ is of full measure under $Q_\mu^{(\vartheta,\tau,\sigma)}$.

Proof. Accept Conjectures 8.1 and 8.2 for parameters (ϑ,τ,σ) under consideration.

1) Since by Proposition 3.2 b) the empirical distribution functions $\widehat{H}_n$ associated to interspike times

$$(\tau_2 - \tau_1, \ldots, \tau_{n+1} - \tau_n) \quad , \quad n \to \infty$$

converge almost surely under $(\vartheta, \tau, \sigma)$, uniformly on $[0, \infty)$, to a limit distribution function $H^{(\vartheta, \tau, \sigma)}$, continuity and strict monotonicity of the limit –stated in Conjecture 8.1– imply almost sure convergence of α-quantiles, $0 < \alpha < 1$. The same assertion then holds for empirical distribution functions associated to interspike times (5.2) observed up to time T_1

$$(\tau_2 - \tau_1, \ldots, \tau_{N_{T_1}} - \tau_{N_{T_1}-1}) \quad , \quad T_1 \to \infty$$

with the same limit distribution function $H^{(\vartheta, \tau, \sigma)}$. As a consequence, we have almost sure convergence of α-quantiles in data sets (5.2) to those of $H^{(\vartheta, \tau, \sigma)}$. In particular, with notations (5.2)–(5.3),

$$\Delta(T_1) \longrightarrow \Delta^{(\vartheta, \tau, \sigma)} \quad , \quad \mathbf{r}(\alpha, T_1) \longrightarrow \mathbf{r}^{(\vartheta, \tau, \sigma)}(\alpha) \tag{8.1}$$

converge almost surely as $T_1 \to \infty$; in the limit appear the corresponding quantities defined from the limit distribution $H^{(\vartheta, \tau, \sigma)}$.

2) Accepting Conjecture 8.2, we have

$$\mathbf{r}^{(\vartheta, \tau, \sigma)}(0.05) < 0.3 \quad , \quad \mathbf{r}^{(\vartheta, \tau, \sigma)}(0.1) < 0.2 \quad , \quad \mathbf{r}^{(\vartheta, \tau, \sigma)}(0.25) < 0.1.$$

In virtue of (8.1), as $T_1 \in \mathbb{N}$ and $T_1 \to \infty$, we do have

$$\mathbf{r}(0.05, T_1) \leq 0.3 \quad , \quad \mathbf{r}(0.1, T_1) \leq 0.2 \quad , \quad \mathbf{r}(0.25, T_1) \leq 0.1 \tag{8.2}$$

for eventually all $T_1 \in \mathbb{N}$. Similarly, accepting Conjecture 8.2 we have

$$\left| E_\mu^{(\vartheta, \tau, \sigma)}(N_1) \Delta^{(\vartheta, \tau, \sigma)} - 1 \right| < 0.05$$

for the limit distribution $H^{(\vartheta, \tau, \sigma)}$, and thus, combining (8.1) with Proposition 3.4,

$$\left| \frac{N_{T_1} \Delta(T_1)}{T_1} - 1 \right| \leq 0.05 \tag{8.3}$$

for eventually all $T_1 \in \mathbb{N}$. By definition of the events $R(T_1) \in \mathcal{G}_{T_1}$ in Definition 5.1 and by Proposition 3.2 a) , the assertion is proved.

$$\square$$

Remark 8.4. By (8.1), Conjecture 8.1 implies that for all $(\vartheta, \tau, \sigma)$, the random variables (5.7)

$$\sum_{j \geq 0} e^{-c_1 \Delta(T_1) j} = \frac{1}{1 - e^{-c_1 \Delta(T_1)}} \quad , \quad \sum_{j \geq 0} e^{-c_1 \Delta(T_1)(j+1)} = \frac{e^{-c_1 \Delta(T_1)}}{1 - e^{-c_1 \Delta(T_1)}}$$

converge almost surely as $T_1 \to \infty$ to the deterministic limits

$$\sum_{j \geq 0} e^{-c_1 \Delta^{(\vartheta, \tau, \sigma)} j} = \frac{1}{1 - e^{-c_1 \Delta^{(\vartheta, \tau, \sigma)}}} \quad , \quad \sum_{j \geq 0} e^{-c_1 \Delta^{(\vartheta, \tau, \sigma)}(j+1)} = \frac{e^{-c_1 \Delta^{(\vartheta, \tau, \sigma)}}}{1 - e^{-c_1 \Delta^{(\vartheta, \tau, \sigma)}}} \tag{8.4}$$

defined in terms of the median of the limit distribution $H^{(\vartheta, \tau, \sigma)}$.

Remark 8.5. Assume that $(\vartheta, \tau, \sigma)$ satisfies Conjectures 8.1 and 8.2. Then, for every $L \in \mathbb{N}$ fixed, the limit distribution function $G_\mu^{(\vartheta,\tau,\sigma)}$ on $[0,\infty)^L$ from Theorem 3.5, almost sure limit of empirical distribution functions $\widehat{G}_m$ associated to the first m L-tuples out of

$$(\tau_{n+1} - \tau_n, \ldots, \tau_{n+L} - \tau_{n+L-1}) \quad , \quad n \in \mathbb{N}$$

as $m \to \infty$, is concentrated on neighbourhoods of the point

$$\left(\Delta^{(\vartheta,\tau,\sigma)}, \ldots, \Delta^{(\vartheta,\tau,\sigma)}\right) \in [0,\infty)^L$$

in the sense that marginals, i.e. image measures under projection on single coordinates $i \in \{1, \ldots, L\}$, admit $\Delta^{(\vartheta,\tau,\sigma)}$ as their median and bounds

$$\mathbf{r}^{(\vartheta,\tau,\sigma)}(0.05) < 0.3, \mathbf{r}^{(\vartheta,\tau,\sigma)}(0.1) < 0.2, \mathbf{r}^{(\vartheta,\tau,\sigma)}(0.25) < 0.1$$

on ratios of distances between upper and lower quantiles divided by the median. To see this, it is sufficient to note that necessarily every marginal of the law $G_\mu^{(\vartheta,\tau,\sigma)}$ in Theorem 3.5 coincides with the probability measure $H^{(\vartheta,\tau,\sigma)}$ of Proposition 3.2 b) .

Remark 8.6. Grant Conjectures 8.1 and 8.2 for $(\vartheta, \tau, \sigma)$. Then

a) expressions (8.4) provide deterministic benchmarks for the location of $(U_{\tau_\ell}, U_{\tau_{(\ell+1)-}})$ to be observed under $(\vartheta, \tau, \sigma)$ in the long run as $\ell \to \infty$,

b) expressions (5.7) provide $\mathcal{G}_{T_1}$-measurable approximations to (8.4), converging to (8.4) as $T_1 \to \infty$.

Proof. i) Note first that the sequence of local maxima $(U_{\tau_\ell})_\ell$ in the output process U is bounded: interspike times being bounded away from 0 by definition in (3.10), so local maxima of U –using (3.16)– take values in the compact set $K := \left[1, \sum_{j \geq 0} e^{-c_1 j \delta_0}\right]$.

ii) For arbitrary $\ell, n, m \in \mathbb{N}$ we have $U_{\tau_\ell} = \sum_{j=1}^{\ell} e^{-c_1(\tau_\ell - \tau_j)}$ and thus

$$U_{\tau_{n+m}} = U_{\tau_n} e^{-c_1(\tau_{n+m} - \tau_n)} + \sum_{j=1}^{m} e^{-c_1(\tau_{n+m} - \tau_{n+j})}. \tag{8.5}$$

If for L large enough an L-tuple of interspike times as considered in Remark 8.5

$$(\tau_{n+1} - \tau_n, \ldots \tau_{n+L} - \tau_{n+L-1}) \quad , \quad n \in \mathbb{N}$$

is well concentrated at $\Delta^{(\vartheta,\tau,\sigma)}$, then values of $U_{\tau_{n+L}}$ will be close to

$$u_\infty^{(\vartheta,\tau,\sigma)} := \sum_{j \geq 0} e^{-c_1 j \Delta^{(\vartheta,\tau,\sigma)}} = \frac{1}{1 - e^{-c_1 \Delta^{(\vartheta,\tau,\sigma)}}}$$

no matter where U_{τ_n} was located in K. Hence small neighbourhoods of $u_\infty^{(\vartheta,\tau,\sigma)}$ are attainable for the process $(U_{\tau_\ell})_\ell$ of local maxima of the output process.

iii) Whenever U_{τ_n} in (8.5) is close to $u_\infty^{(\vartheta,\tau,\sigma)}$ for some n, an L-tuple of interspike times well concentrated at $\Delta^{(\vartheta,\tau,\sigma)}$ as in ii) allows to write in good approximation

$$U_{\tau_{n+L}} \approx u_\infty^{(\vartheta,\tau,\sigma)} e^{-c_1 L \Delta^{(\vartheta,\tau,\sigma)}} + \sum_{j=1}^{L} e^{-c_1(L-j)\Delta^{(\vartheta,\tau,\sigma)}} = u_\infty^{(\vartheta,\tau,\sigma)}.$$

Hence also $U_{\tau_{n+L}}$ will be close to $u_\infty^{(\vartheta,\tau,\sigma)}$. This shows that small neighbourhoods of $u_\infty^{(\vartheta,\tau,\sigma)}$ will be attained infinitely often by the process of local maxima in the long run.

iv) Thus asymptotically as $\ell \to \infty$, pairs $\left(U_{\tau_\ell}, U_{(\tau_{\ell+1})^-}\right)$ will visit small neighbourhoods of

$$\left(u_\infty^{(\vartheta,\tau,\sigma)}, u_\infty^{(\vartheta,\tau,\sigma)} e^{-c_1 \Delta^{(\vartheta,\tau,\sigma)}}\right) = \left(\frac{1}{1 - e^{-c_1 \Delta^{(\vartheta,\tau,\sigma)}}}, \frac{e^{-c_1 \Delta^{(\vartheta,\tau,\sigma)}}}{1 - e^{-c_1 \Delta^{(\vartheta,\tau,\sigma)}}}\right)$$

infinitely often. In this sense, the deterministic expression (8.4) provides a benchmark for the location of pairs $\left(U_{\tau_\ell}, U_{(\tau_{\ell+1})^-}\right)$ under $(\vartheta, \tau, \sigma)$ in the long run as $\ell \to \infty$, in virtue of our two conjectures. This is a). By (8.1), $\Delta(T_1)$ converges to $\Delta^{(\vartheta,\tau,\sigma)}$ almost surely as $T_1 \to \infty$. So if we have observed the stochastic neuron up to time T_1, for T_1 large enough, expressions (5.7)

$$\left(\frac{1}{1 - e^{-c_1 \Delta(T_1)}}, \frac{e^{-c_1 \Delta(T_1)}}{1 - e^{-c_1 \Delta(T_1)}}\right)$$

are $\mathcal{G}_{T_1}$-measurable approximations to the benchmark in (8.4). This is b). □

References

[1] Jacques Azéma, Marie Duflo, and Daniel Revuz, *Mesure invariante des processus de Markov récurrents*, Séminaire de Probabilités, III (Univ. Strasbourg, 1967/68), Springer LNM 88, Berlin, 1969, pp. 24–33. MR-0260014

[2] Pierre Brémaud, *Point processes and queues*, Martingale dynamics, Springer Series in Statistics, Springer-Verlag, New York-Berlin, 1981. MR-636252

[3] Raphaël Cerf, Paolo Dai Pra, Marco Formentin, and Daniele Tovazzi, *Rhythmic behavior of an Ising model with dissipation at low temperature*, ALEA Lat. Am. J. Probab. Math. Stat. **18** (2021), no. 1, 439–467, doi. MR-4219671

[4] Susanne Ditlevsen and Eva Löcherbach, *Multi-class oscillating systems of interacting neurons*, Stochastic Process. Appl. **127** (2017), no. 6, 1840–1869, doi. MR-3646433

[5] G. Bard Ermentrout and David H. Terman, *Mathematical foundations of neuroscience*, Interdisciplinary Applied Mathematics, vol. 35, Springer, New York, 2010, doi. MR-2674516

[6] Alan L Hodgkin and Andrew F Huxley, *A quantitative description of membrane current and its application to conduction and excitation in nerve*, The Journal of physiology **117** (1952), no. 4, 500–544.

[7] Simon Holbach, *Positive Harris recurrence for degenerate diffusions with internal variables and randomly perturbed time-periodic input*, Stochastic Process. Appl. **130** (2020), no. 11, 6965–7003, doi. MR-4158809

[8] Reinhard Höpfner, *Polynomials under Ornstein-Uhlenbeck noise and an application to inference in stochastic Hodgkin-Huxley systems*, Stat. Inference Stoch. Process. **24** (2021), no. 1, 35–59, doi. MR-4236595

[9] Reinhard Höpfner and Yury Kutoyants, *Estimating discontinuous periodic signals in a time inhomogeneous diffusion*, Stat. Inference Stoch. Process. **13** (2010), no. 3, 193–230, doi. MR-2729649

[10] Reinhard Höpfner and Eva Löcherbach, *Limit theorems for null recurrent Markov processes*, Mem. Amer. Math. Soc. **161** (2003), no. 768, vi+92, doi. MR-1949295

[11] Reinhard Höpfner, Eva Löcherbach, and Michèle Thieullen, *Ergodicity and limit theorems for degenerate diffusions with time periodic drift. Application to a stochastic Hodgkin-Huxley model*, ESAIM Probab. Stat. **20** (2016), 527–554, doi. MR-3581833

[12] Reinhard Höpfner, Eva Löcherbach, and Michèle Thieullen, *Ergodicity for a stochastic Hodgkin-Huxley model driven by Ornstein-Uhlenbeck type input*, Ann. Inst. Henri Poincaré Probab. Stat. **52** (2016), no. 1, 483–501, doi. MR-3449311

[13] ⸻, *Strongly degenerate time inhomogeneous SDEs: densities and support properties. Application to Hodgkin-Huxley type systems*, Bernoulli **23** (2017), no. 4A, 2587–2616, doi. MR-3648039

[14] Cédric Hummel, *Netzwerke von Hodgkin-Huxley Neuronen*, Institut für Mathematik, Universität Mainz, Masterarbeit (2019).

[15] Eugene M. Izhikevich, *Dynamical systems in neuroscience: the geometry of excitability and bursting*, Computational Neuroscience, MIT Press, Cambridge, MA, 2007. MR-2263523

[16] Jean Jacod and Albert N. Shiryaev, *Limit theorems for stochastic processes*, Grundlehren der mathematischen Wissenschaften [Fundamental Principles of Mathematical Sciences], vol. 288, Springer-Verlag, Berlin, 1987, doi. MR-959133

[17] Eva Löcherbach and Dasha Loukianova, *On Nummelin splitting for continuous time Harris recurrent Markov processes and application to kernel estimation for multi-dimensional diffusions*, Stochastic Process. Appl. **118** (2008), no. 8, 1301–1321, doi. MR-2427041

[18] Michel Métivier, *Semimartingales*, A course on stochastic processes, de Gruyter Studies in Mathematics, vol. 2, Walter de Gruyter & Co., Berlin-New York, 1982. MR-688144

[19] Esa Nummelin, *A splitting technique for Harris recurrent Markov chains*, Z. Wahrsch. Verw. Gebiete **43** (1978), no. 4, 309–318, doi. MR-0501353

[20] _____, *General irreducible Markov chains and nonnegative operators*, Cambridge Tracts in Mathematics, vol. 83, Cambridge University Press, Cambridge, 1984, doi. MR-776608

[21] Daniel Revuz and Marc Yor, *Continuous martingales and Brownian motion*, Grundlehren der mathematischen Wissenschaften [Fundamental Principles of Mathematical Sciences], vol. 293, Springer-Verlag, Berlin, 1991, doi. MR-1083357

[22] John Rinzel and Robert N. Miller, *Numerical calculation of stable and unstable periodic solutions to the Hodgkin-Huxley equations*, Math. Biosci. **49** (1980), no. 1-2, 27–59, doi. MR-572841

[23] Hermann Witting, *Mathematische Statistik. I*, Parametrische Verfahren bei festem Stichprobenumfang. [Parametric methods for fixed sample size], B. G. Teubner, Stuttgart, 1985, doi. MR-943833

[24] Hermann Witting and Ulrich Müller-Funk, *Mathematische Statistik. II*, Asymptotische Statistik: parametrische Modelle und nichtparametrische Funktionale. [Asymptotic statistics: parametric models and nonparametric functionals], B. G. Teubner, Stuttgart, 1995, doi. MR-1363716